The Discrete Element Method and Its Use in Physical Modeling

Jerome B. Johnson
Institute of Northern Engineering
University of Alaska Fairbanks

xTerramechanics Workshop, Keck Institute for Space Studies,
California Institute of Technology, June 22, 2011

Contributors

- J. Peters, J. Wibowo, R. Kala, D. Horner - US Army Corps of Engineers, Engineer Research and Development Center, Vicksburg, MS
- D. Cole, M. Hopkins, K. Knuth - US Army Corps of Engineers, Engineer Research and Development Center, Hanover, NH
- M. Muthuswamy, A. Tordesillas - Department of Mathematics and Statistics, University of Melbourne, 3010, Australia
- R. Sullivan - Space Sciences, Cornell University, Ithaca, NY
- A. Kulchitshy, J. Johnson, University of Alaska – Fairbanks
- L. Taylor – Planetary Geosciences Institute Department of Earth & Planetary Sciences, University of Tennessee

UAF INE

Outline Of Presentation

- The discrete element method (DEM)
  - What is it and why use it over other simulation methods
  - Strengths and weakness of the method
  - What are the DEM parameters
  - What is a physical DEM and how do we achieve it.
- Bounding the problem space and progressing toward a physical DEM
- Case example and example prediction to win a beer from José (hopefully)

UAF INE

Discrete Element Method (DEM)

- Replicate soil particulate nature
- Large-scale deformation/failure of particle aggregate
- Incorporate test geometry
- Slip planes and separations form between groups of particles, capturing evolving structure/failure mechanisms

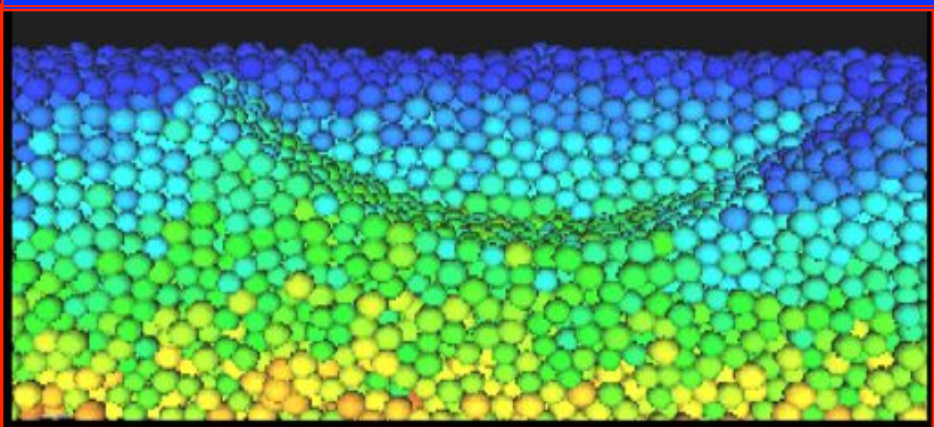

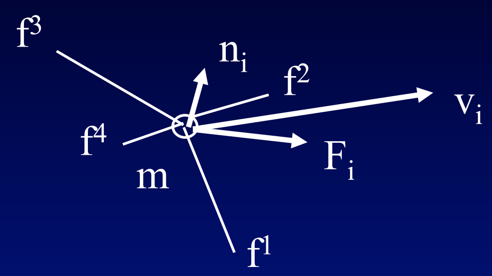

Forces Acting on Particle k

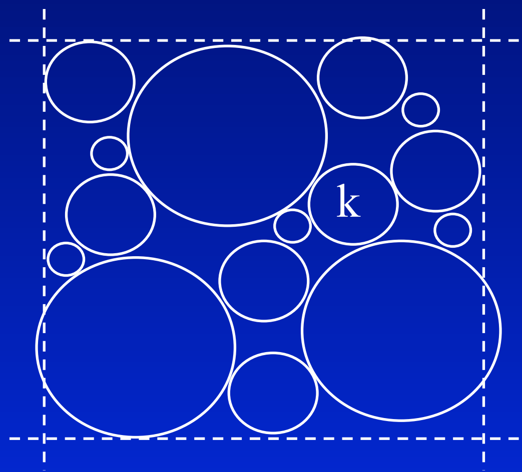

Discrete Particle System

Why DEM Instead of Continuum?

- Continuum material behavior descriptions combine multiple physical processes into complex functions that are difficult to apply to natural (variable & inhomogeneous materials)
- Explicitly describes the dynamics of assemblies of particles and the micro-mechanical interaction processes between grains – including inhomogeneity
- The evolution of scale-dependant material state during failure and large-scale deformation is determined through "simple" grain-to-grain interaction mechanics

DEM Strengths & Weaknesses

- Strengths
  - Interactions are at the grain scale – where all the action for soil deformation occurs
  - Explicit algorithms for separate physical dynamic or quasi-static processes
  - Complex behavior is captured through the separately acting physical process algorithms
  - Results constitute a virtual experiment
  - Can be combined with other numerical methods to solve potential problems (e.g. Lattice Boltzman)
- Weaknesses
  - Computationally expensive
  - Conducting experiments to define grain properties and contact mechanics is complex and difficult
  - Constructing realistic DEM particle beds is difficult

DEM Parameters

- Physical Parameters
  - Particle size, shape, specific gravity, contact area radius
  - Dilating sphere radius
- Mechanical parameters
  - Contact friction coefficient
  - Normal contact stiffness
  - Contact tensile strength, creep viscosity, normal viscosity (for bonded particles)
- Other
  - Gravity
  - Porosity/density (derived quantities)
  - Coordination number (derived)

Physical DEM : An Approach

- Experiments to define grain-to-grain interaction
  - Mechanical properties
  - Particle contact mechanics
  - Physical properties
- Experiments to define macro-scale properties
- Experiments on machine/regolith interaction
- Simulation of all experiments
- Incorporate environmental conditions
  - Surface cleanliness effect (Van der Wals)?
  - Gravity
  - Other
- Simulations have a predictive capability

Forces and Torques

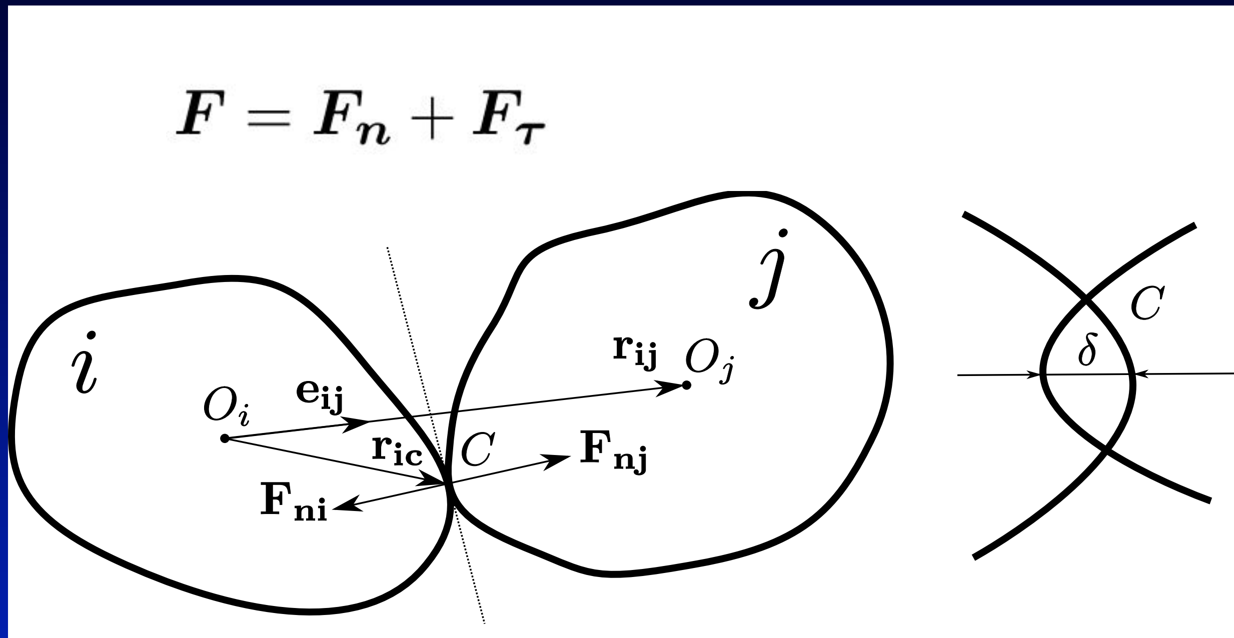

Requires

- Exact Distance/Overlap
- Velocities at Contacts
- Previous Time Step Forces at Contacts
- Storage for Contacts

UAF INE

Contact Detection

Uses bounding boxes of atoms.
Creates the list of atoms that may be in contact.

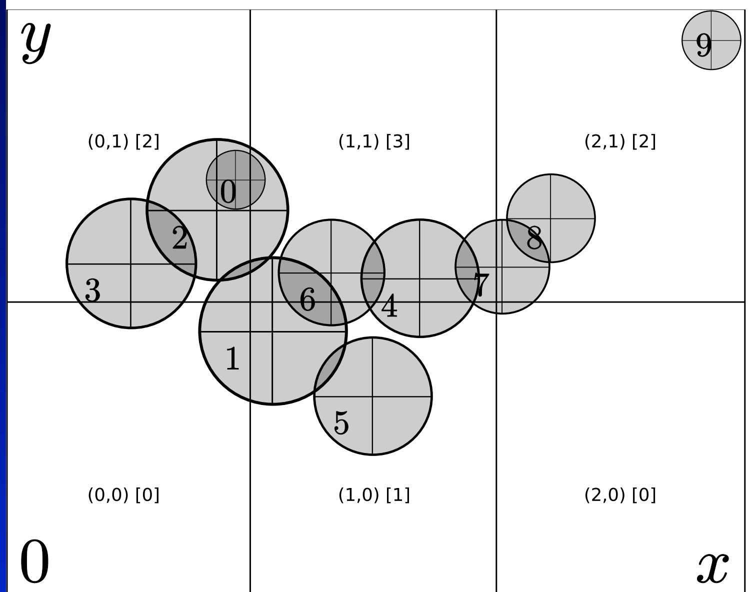

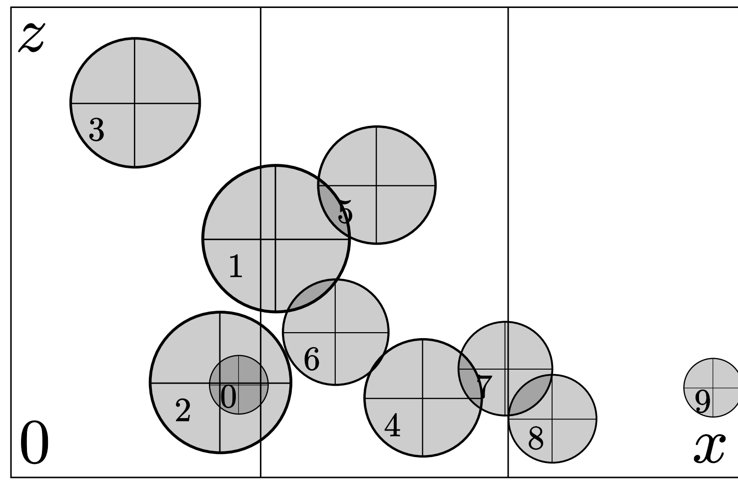

Space partitioning in horizontal plane,
sweep and prune in columns.

Kulchitsky

Collisional Force Model

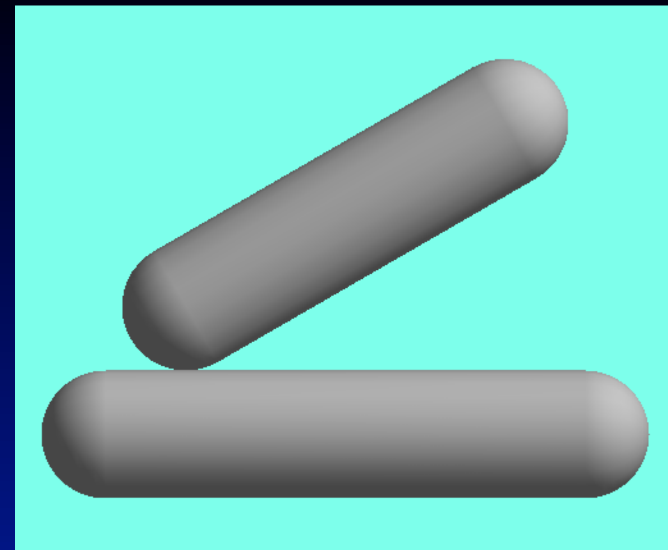

Normal Force:

$$\delta_n^n = \left|\bar{d}\right| - R_1 - R_2$$

$$F_n^n = -\left(k_{ne} A \delta_n^n + k_{nv}\sqrt{A}\,\dot{\delta}_n^{n-1/2}\right)$$

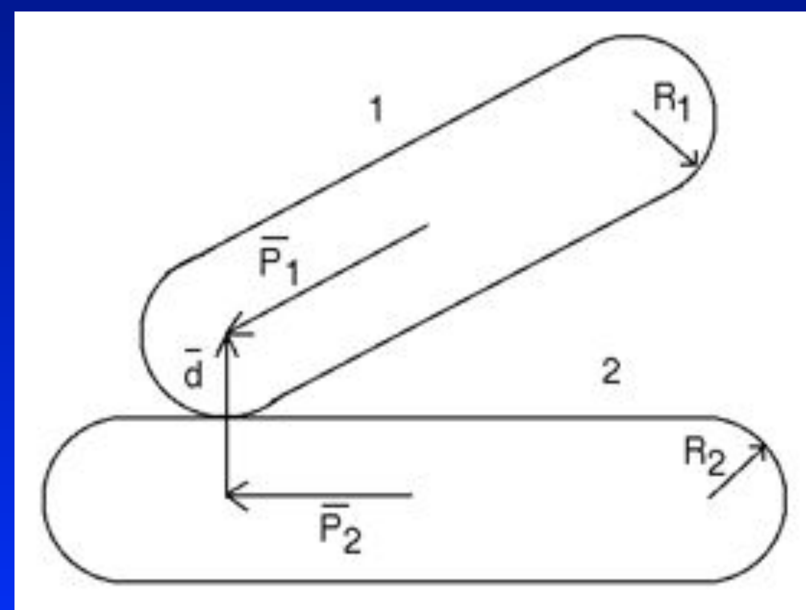

Tangential Force:

$$\bar{F}_{te}^n = \bar{F}_{te}^{n-1} - A k_{te} \Delta t \bar{V}_t^{n-1/2}$$

$$\left|\bar{F}_{te}^n\right| \le \mu F_n^n$$

Frozen Joint Force Model

The d vectors are defined in the body frame of the particle. Initially coincident, relative motion causes the d vectors to diverge. The n vectors are the unit vectors in the d direction. The angle α, the deformation at the center point δ_o, and the strain $\delta(x)$ at a point on the contact plane are given by

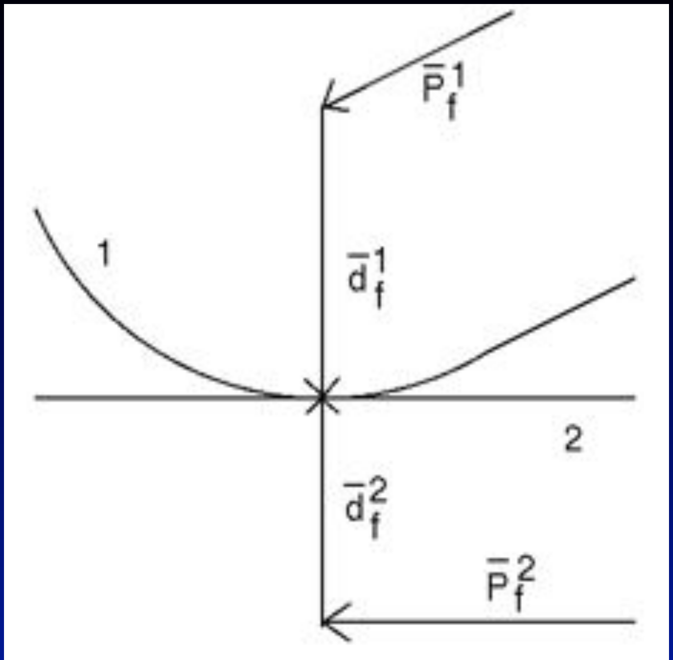

$$\alpha \cong \left| \bar{n}_1 \times -\bar{n}_2 \right|$$

$$\bar{\delta}_o = \bar{X}_2 + \bar{P}_{2f} + \bar{d}_{2f} - \bar{X}_1 - \bar{P}_{1f} - \bar{d}_{1f}$$

$$\delta_n(x) = \bar{\delta}_o \bullet \bar{n}_1 + \alpha x$$

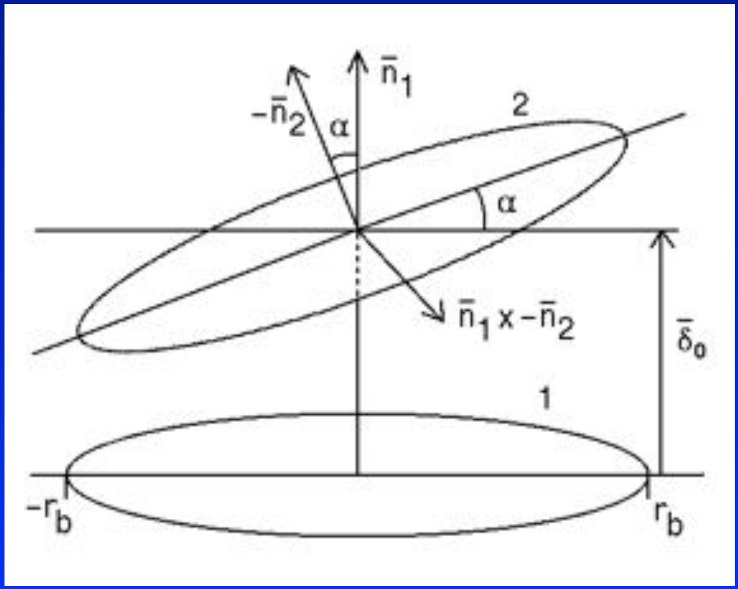

UAF INE

Frozen Joint Force Model (2)

The strain δ(x) between a point on plane 1 and the corresponding point on plane 2 is

$$\delta_n\left(x\right) = \bar{\delta}_o \bullet \bar{n}_1 + \alpha x$$

Integrating the stress over the contact plane yields the normal force with similar expressions for the tangential force and moments.

$$F_{ne} = k_{ne_1} \int_{-r_b}^{+r_b} \delta_n(x)\, y(x)\, dx$$

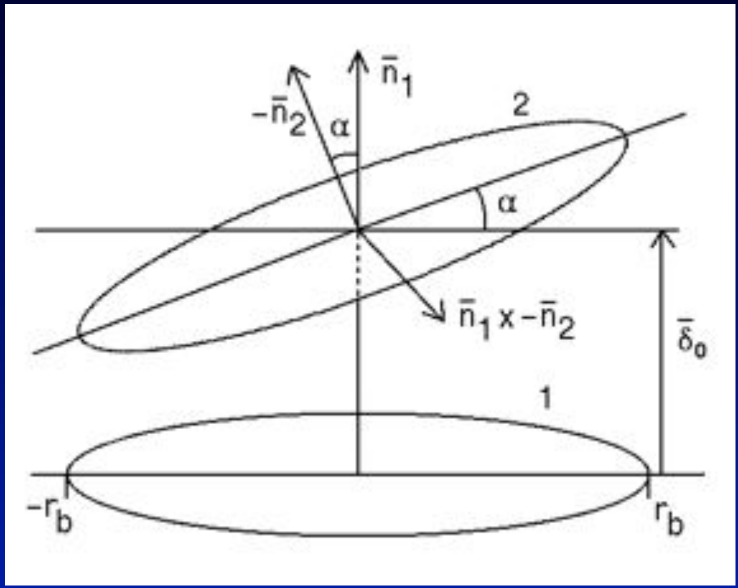

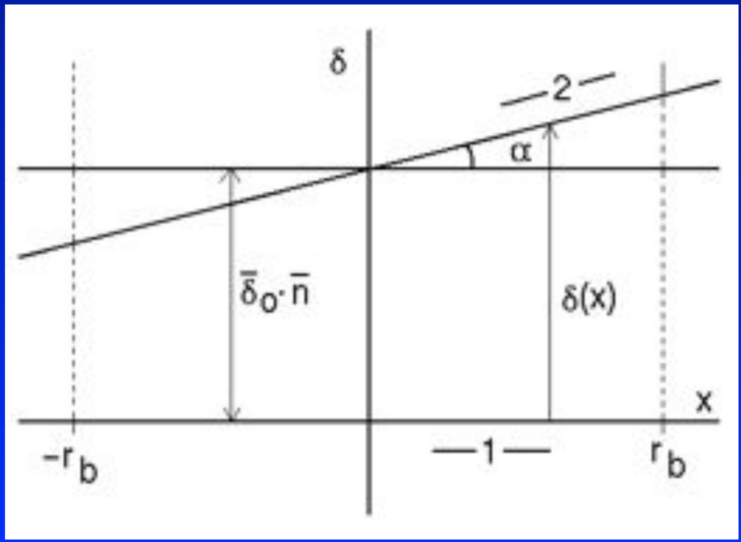

Frozen Joint Fracture Model

Failure in tension. Use a linear elastic constitutive model with strain softening.

$-r_b \le x \le x_1$ is in loading region

$x_1 \le x \le x_2$ is in unloading region

$x_2 \le x$ is in fractured region

Integrating the stress over the contact plane yields the normal force. Similar expressions for tangential force and moments.

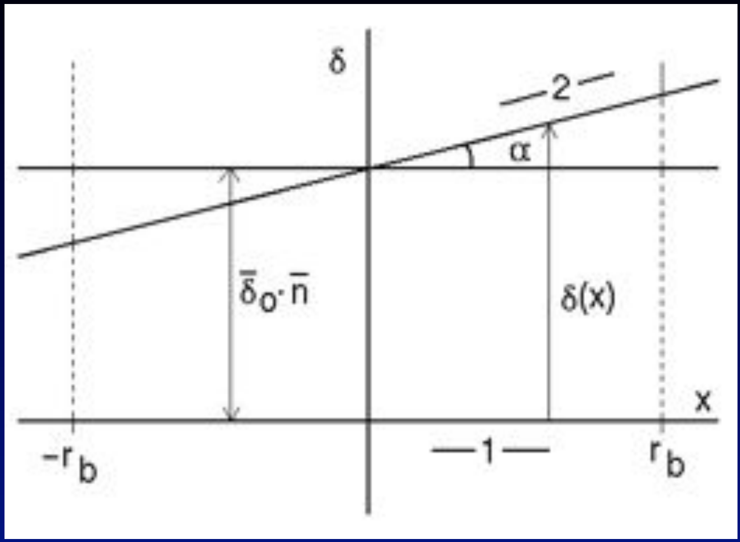

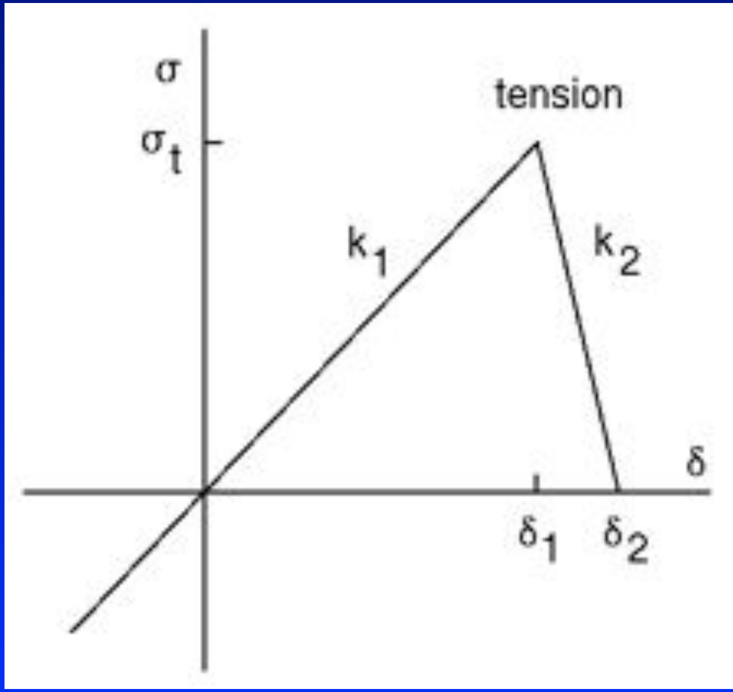

$$F_{ne} = k_{ne_1} \int_{-r_b}^{x_1} \delta_n(x)\, y(x)\, dx + \int_{x_1}^{x_2} \left[\sigma_t - k_{ne_2} (\delta_n(x) - \delta_1) \right] y(x)\, dx$$

Frozen Joint Creep Model

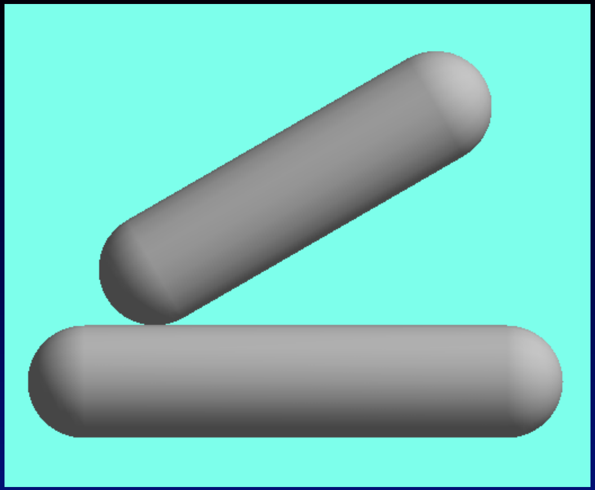

Creep is assumed to diminish the tensile stress in a frozen joint.
Creep moves the displaced d_f toward the current contact d vectors

$$\bar{t}_1 = \bar{P}_1 + \bar{d}_1 - \bar{P}_{1f} - \bar{d}_{1f}$$

$$\Delta\bar{d}_{1f} = \frac{\Delta t}{\eta_c\sqrt{A}}\left[\bar{F}_1\cdot\bar{t}_1 + \bar{M}_1\cdot\left(\bar{n}_1\times\bar{t}_1\right)\right]\bar{t}_1$$

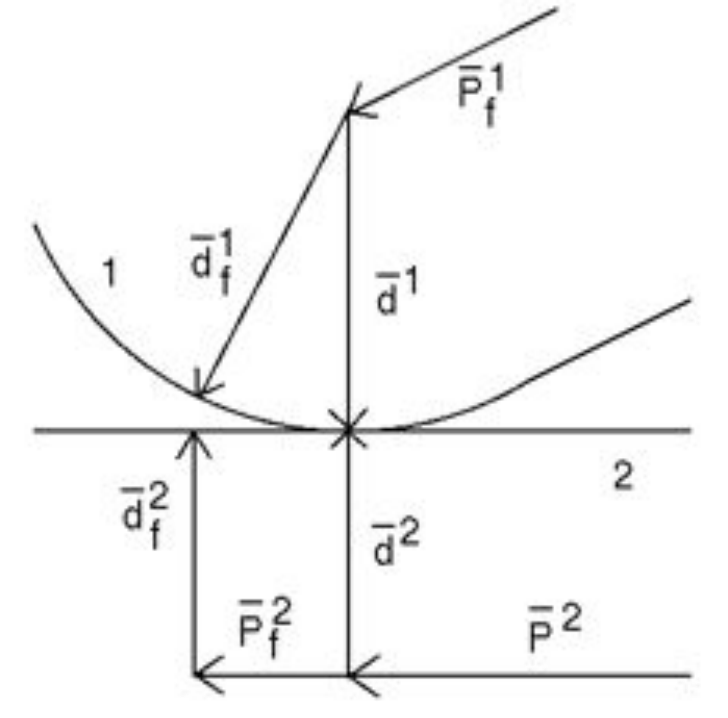

UAF INE

Sintering Model

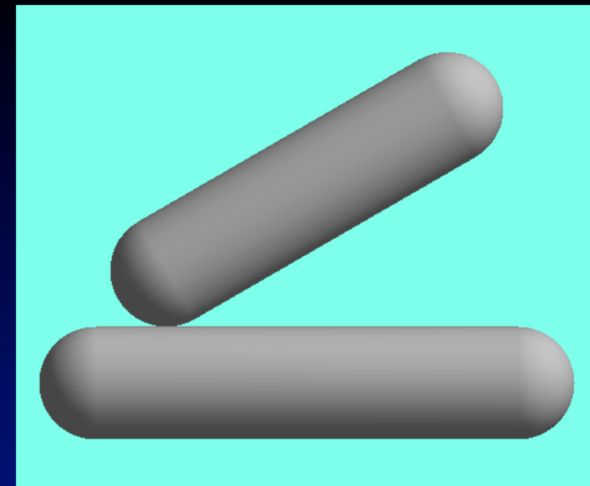

Growth of the bond radius is assumed to have pressure-less and pressure induced components

$$\dot{r}_b = \frac{\left[\frac{4}{3}\pi r_{bt}^2 \dot{r}_{bt} \sin\left(\frac{r_{bt}}{R}\right) - \pi A r_{bt}^3 \left(\frac{3\times 10^{-2}}{2n\pi r_{bt}^2}\right)^n + \pi A r_b^3 \left(\frac{3F_c}{2n\pi r_b^2}\right)^n \right]}{\frac{4}{3}\pi r_b^2 \sin\left(\frac{r_b}{R}\right)}$$

where r_{bt} is empirically derived from Gubler's (1982) data

$$r_{bt} = \sqrt{\frac{q\alpha t^\beta}{\pi\sigma_{ice}}}$$

High Resolution DEM Simulations (HRS)

- HRS are possible on high performance computers (HPC), but take days of CPU effort
- For HRS how many particles is enough?

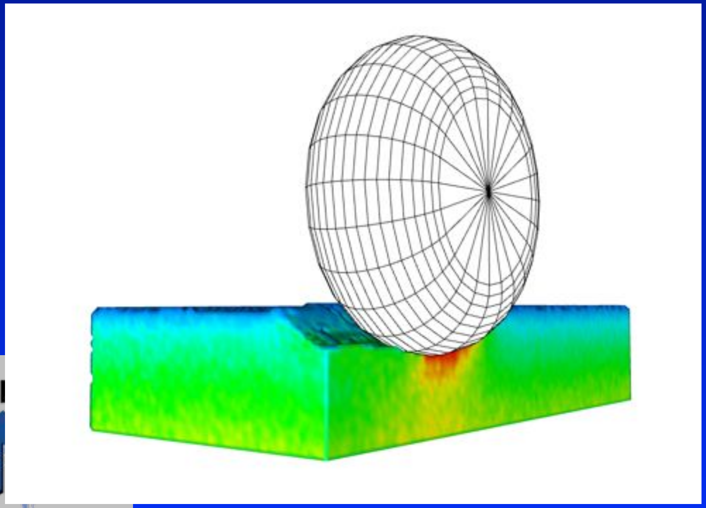

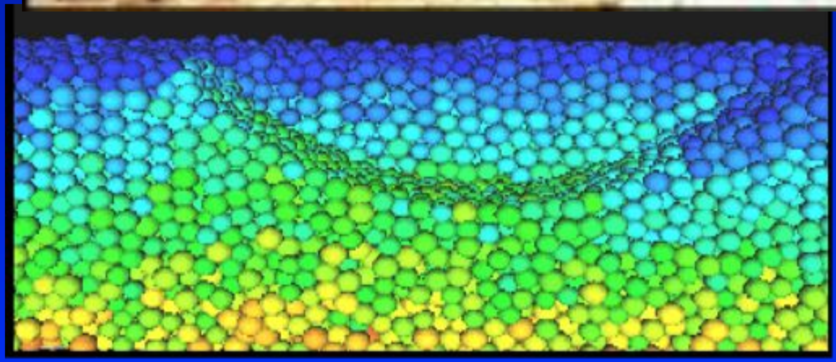

Convergence properties of DEM with a view toward practical applications

Maya Muthuswamy (1), Johannes Wibowo (2), John Peters (2), Raju Kala (2)

Undergraduate Research Supervisor:
Dr Antoinette Tordesillas (1)

(1) Department of Mathematics and Statistics, University of Melbourne, 3010, Australia
(2) US Army Corps of Engineers, Engineer Research and Development Center, Vicksburg, MS

UAF INE

THE UNIVERSITY OF MELBOURNE

Method

- Kept particle size distribution and box/punch ratios constant:
  - Minimum radius: 0.05 in
  - Maximum radius: 0.1 in
  - Ratio of punch-width:height:width = 1:5:10

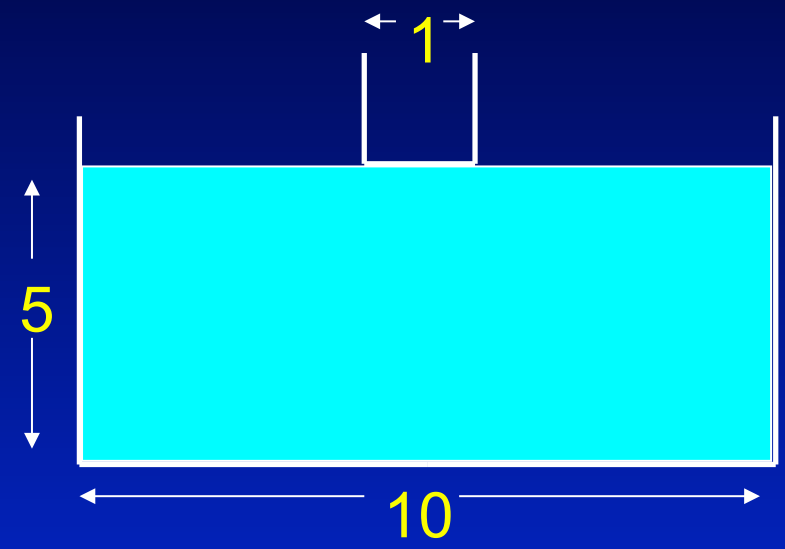

- Varied domain size – label in terms of relative punch size:
  - From Box 1 (2279 particles) to Box 12 (400K particles)
  - Boxes used: 1, 1.5, 2, 3, 4, 6

UAF INE

Project 1: Step 3: Minor principal stress: No gravity: Box 1 (2.3k)

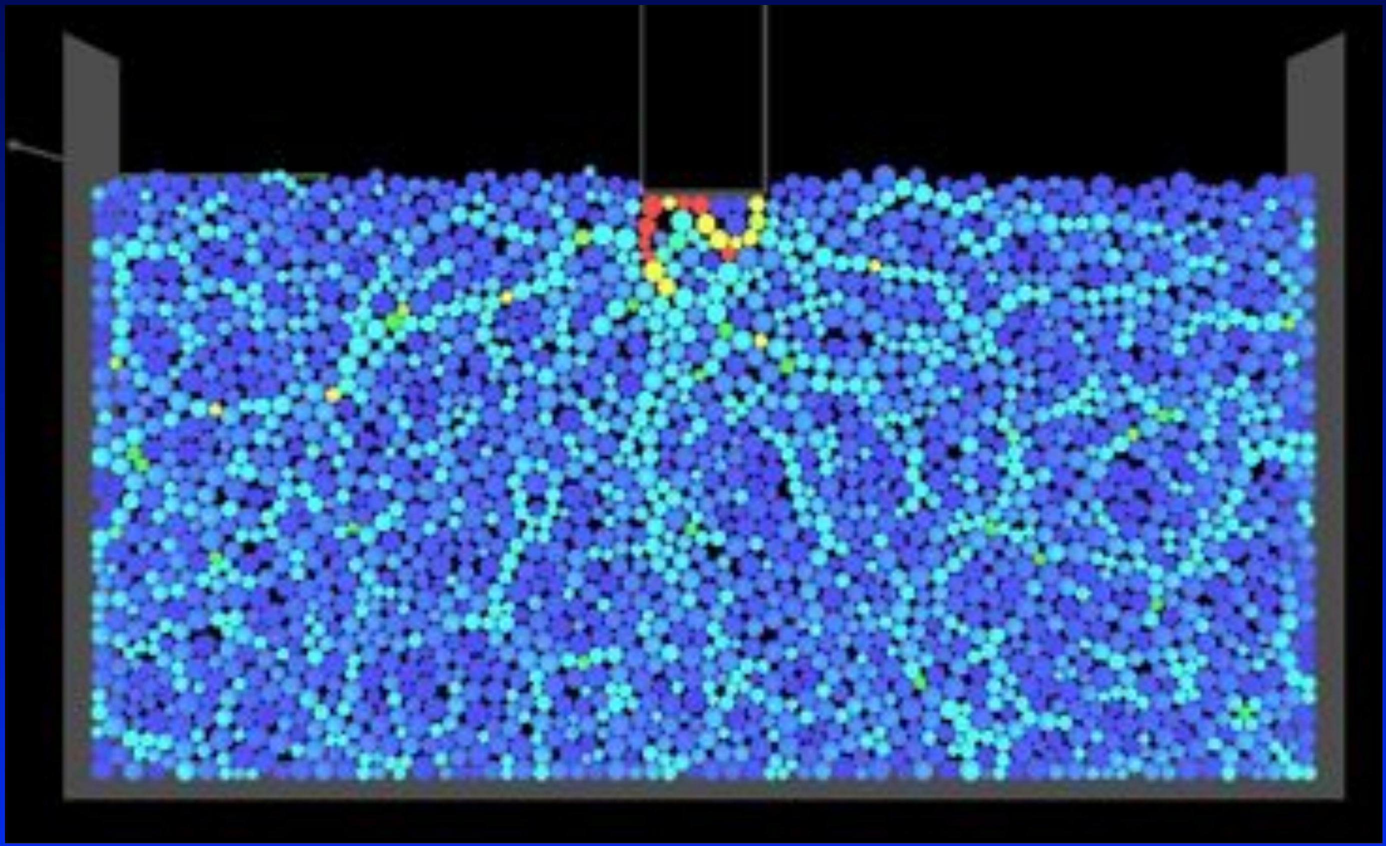

Project 1: Step 3: Minor principal stress: No gravity: Box 1.5 (5.2k)

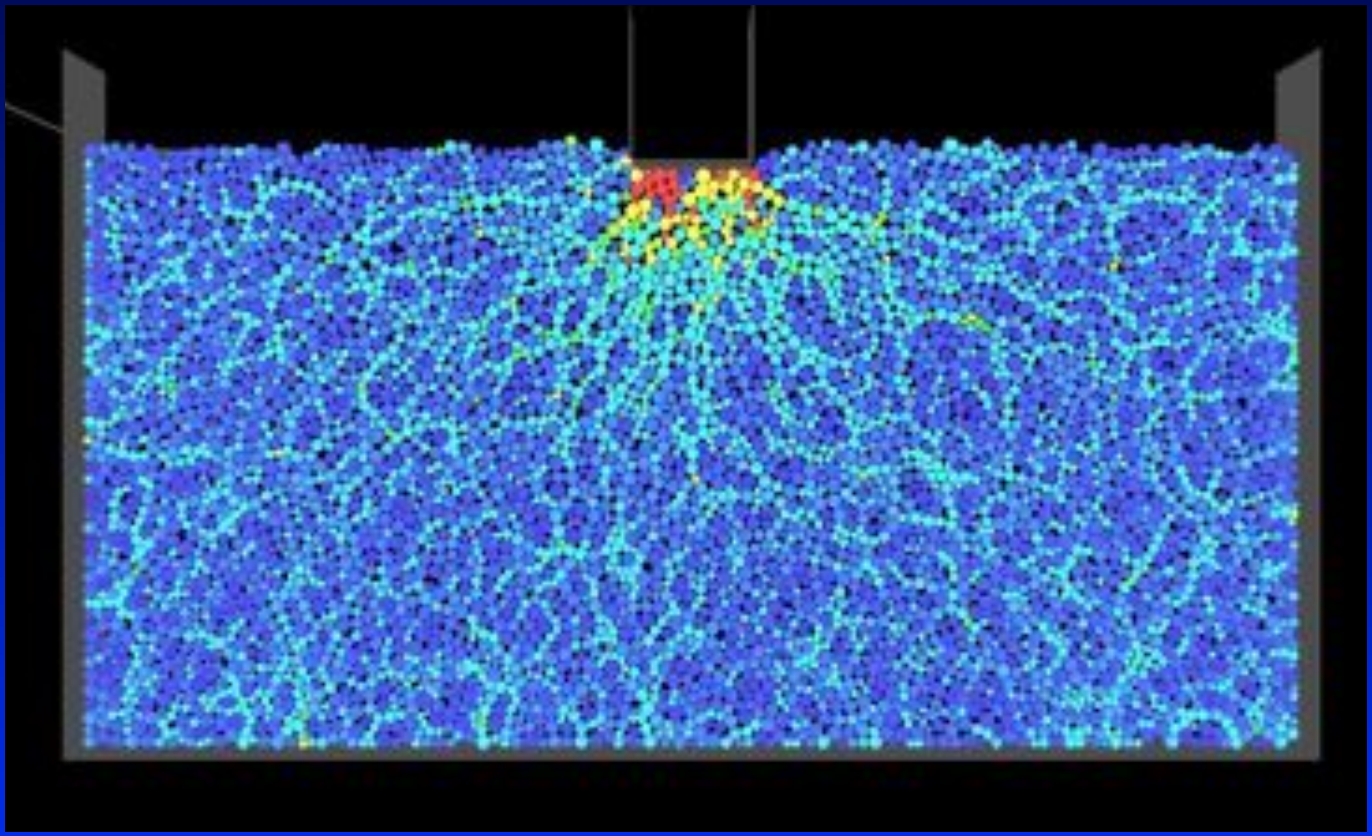

Project 1: Step 3: Minor principal stress: No gravity:

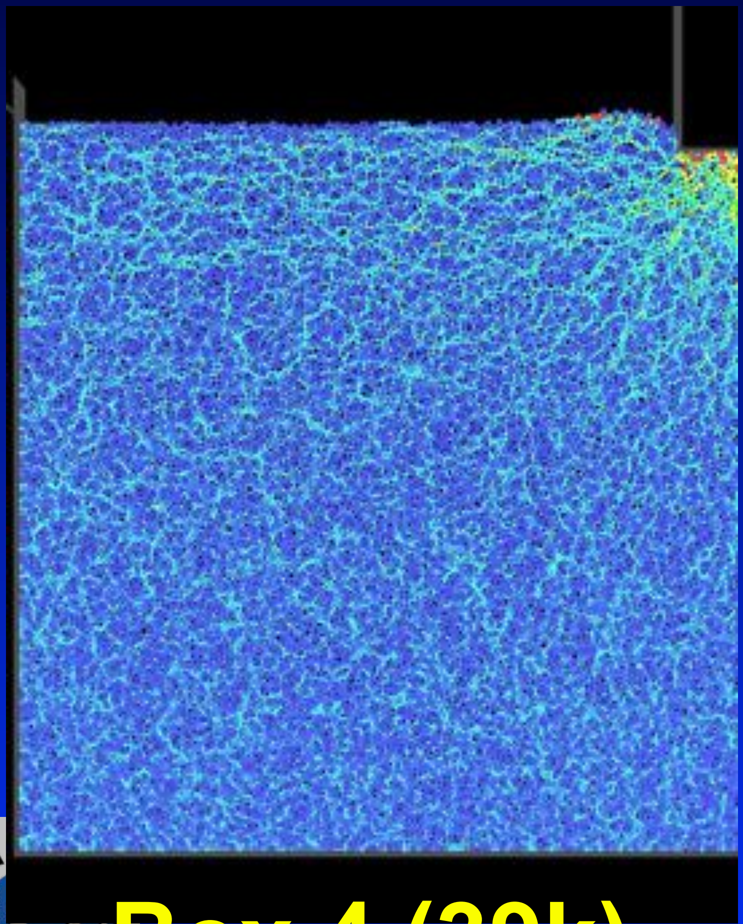

Box 4 (39k)

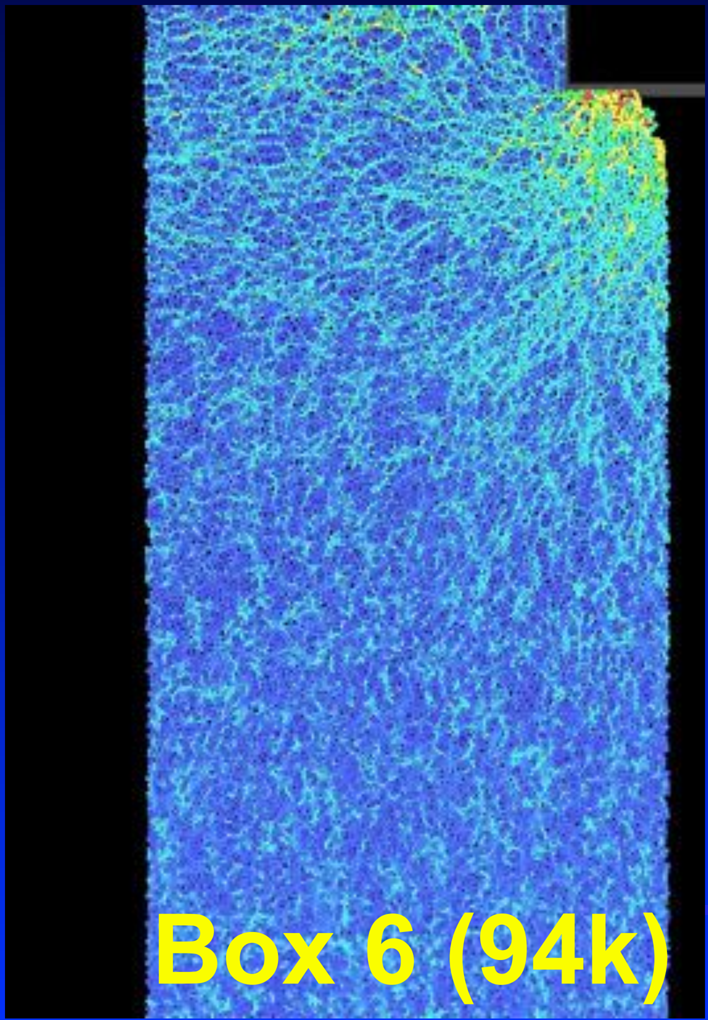

Box 6 (94k)

Project 1: Step 4: Force chain convergence

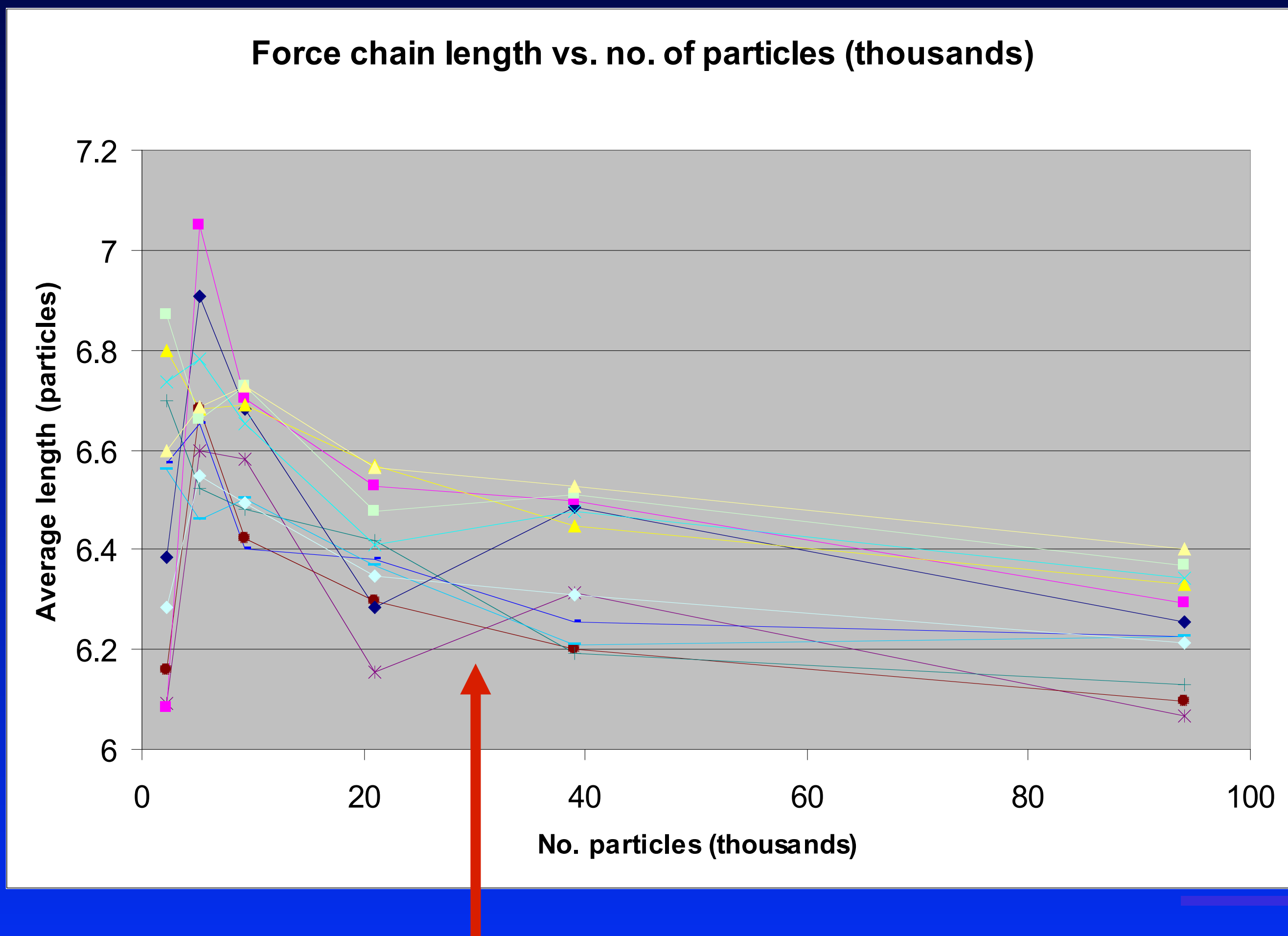

Convergence

Project 2: (4) Particle size

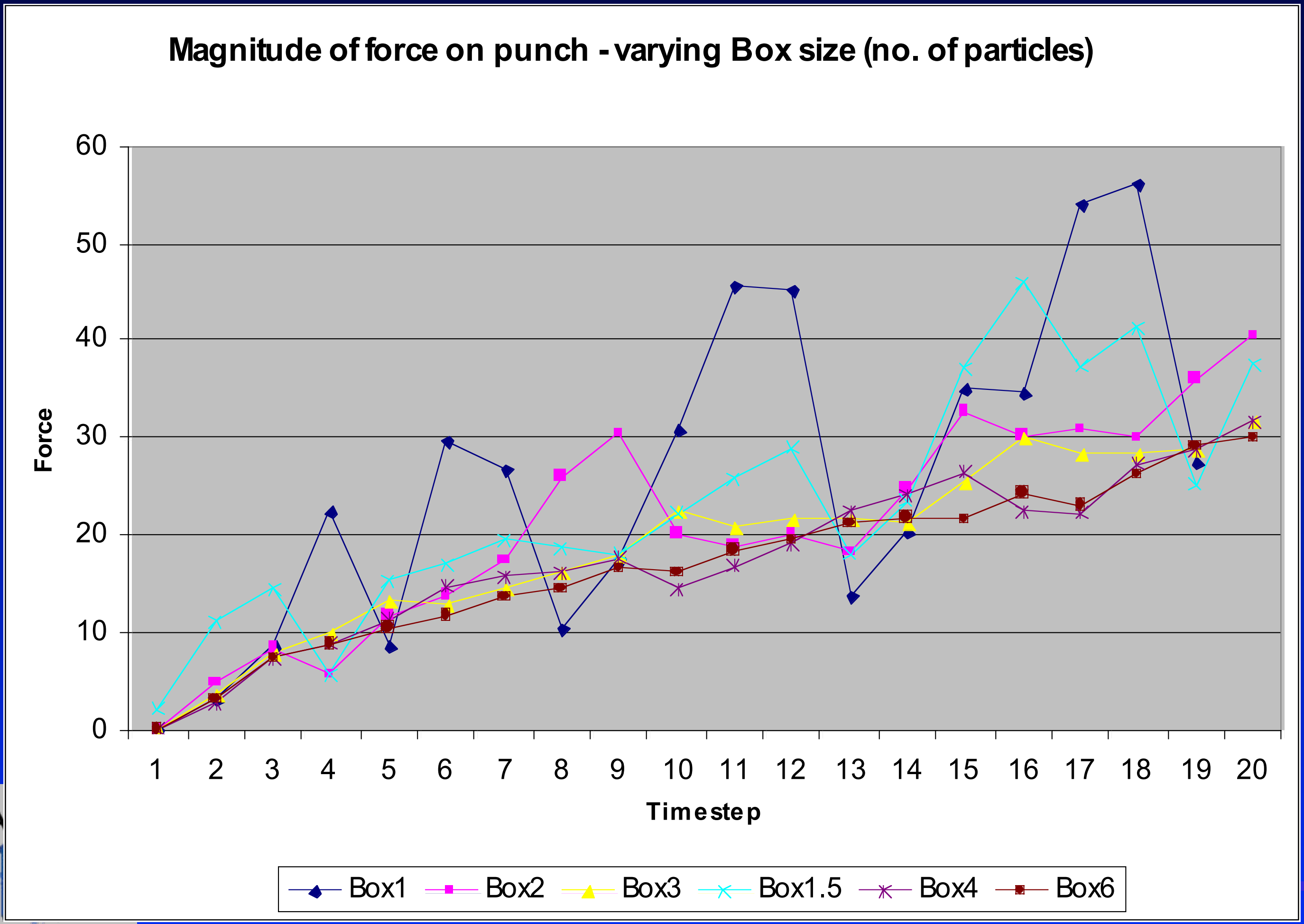

As no. particles increases:

- Load graph becomes smoother/ less random
- Appears to converge at Box 3/4

Project 2: (4) Convergence

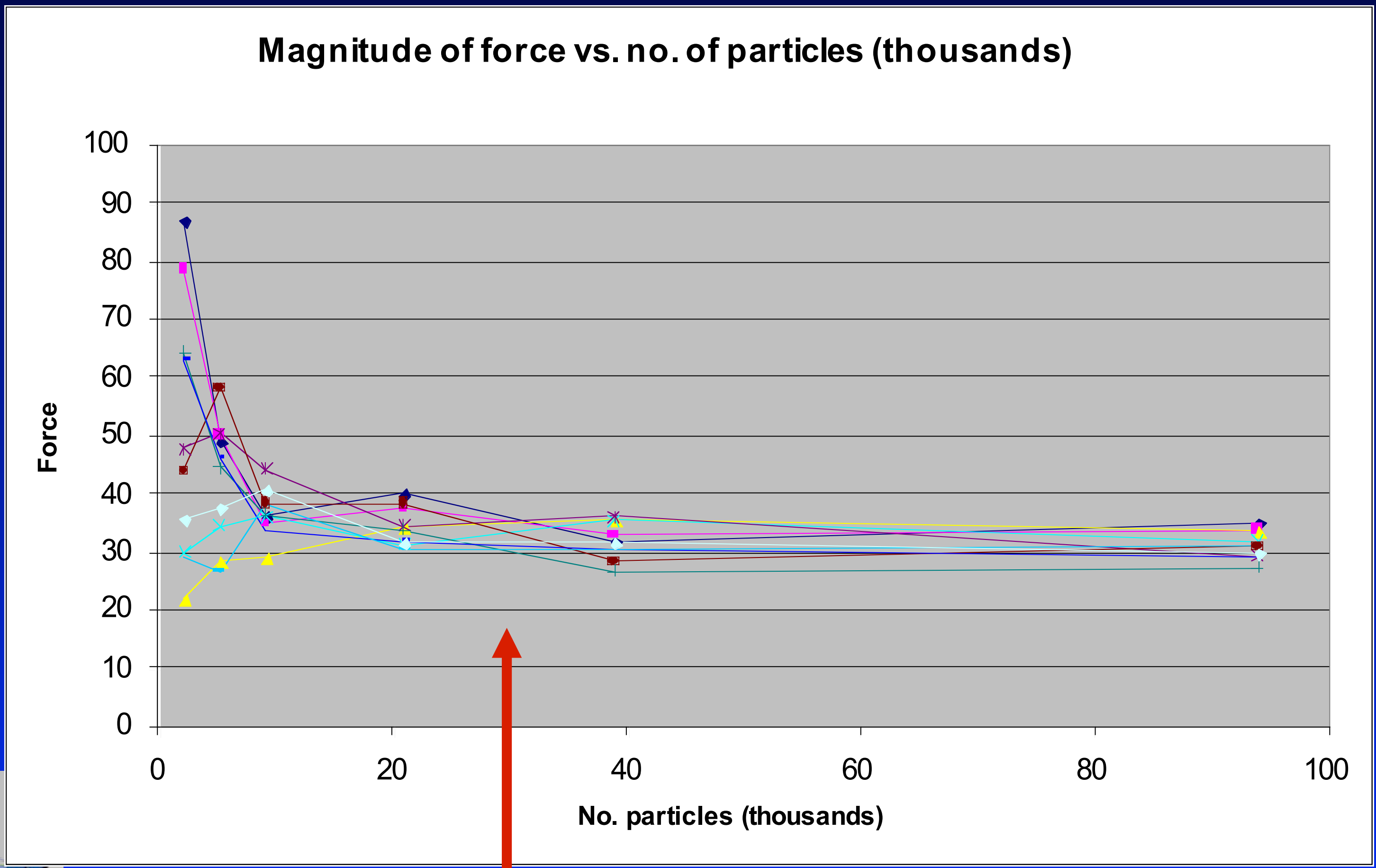

Convergence

Conclusions

- Estimate of required number of particles in 3D:
  - No shear bands: 2D: 30K (230 x 120 particles), so 3D: 230 x 120 x 230 = 6.4 million particles!
  - With shear bands: 2D: 320K (800 x 400 particles), so 3D: 800 x 400 x 800 = 256 million particles!
- Solutions?
  - Invent bigger, faster machines!
  - Develop new contact laws for DEM, taking into account contact information – reducing number of particles needed

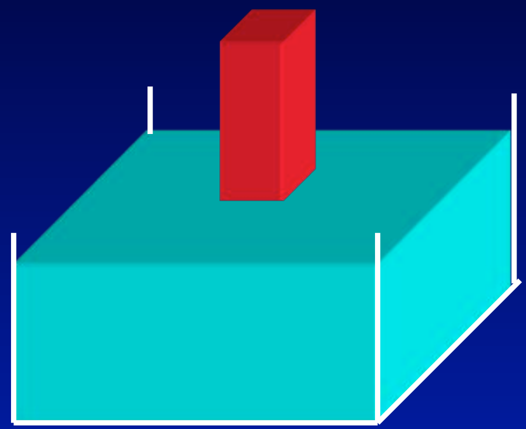

UAF INE

Experiment & Simulation

- Micro-scale grain contact properties
- Tri-axial soil properties tests
- Machine/ soil interaction tests
- Simulation of all tests
- Combined Machine soil interaction test data and tri-axial cell simulation to derive macro-scale soil behavior

UAF INE

Laser07 Project

"Micromechanical experiments and numerical modeling of lunar regolith and its simulants"

D. M. Cole, M.A. Hopkins and L.A. Taylor

Goals:

- Quantify the normal & sliding contact properties of lunar materials & simulants.
- Develop contact laws for implementation in discrete element models & simulate engineering-scale behavior.

Lunar materials:

-Plagioclase with varying degrees of space weathering

-Agglutinates

-Pyroxene

-Volcanic glass beads

Simulants:

-USGS Plagioclase, olivine, pyroxene, chromite

-JSC-1A

-Orbitec agglutinate

D.M. Cole, L.A. Taylor, Y. Liu and M.A. Hopkins (2010) Grain-scale mechanical properties of lunar plagioclase and its simulant: Initial experimental findings and modeling implications. In *Proceedings of ASCE Earth & Space 2010:* Engineering, Science, Construction, and Operations in Challenging Environments, pp. 74 – 83, DOI: 10.1061/41096(366)10

Grain-scale experimental system
– Normal contact behavior –

Actuator (10 N capacity)

Laser sensor (< 0.1 μm resolution)

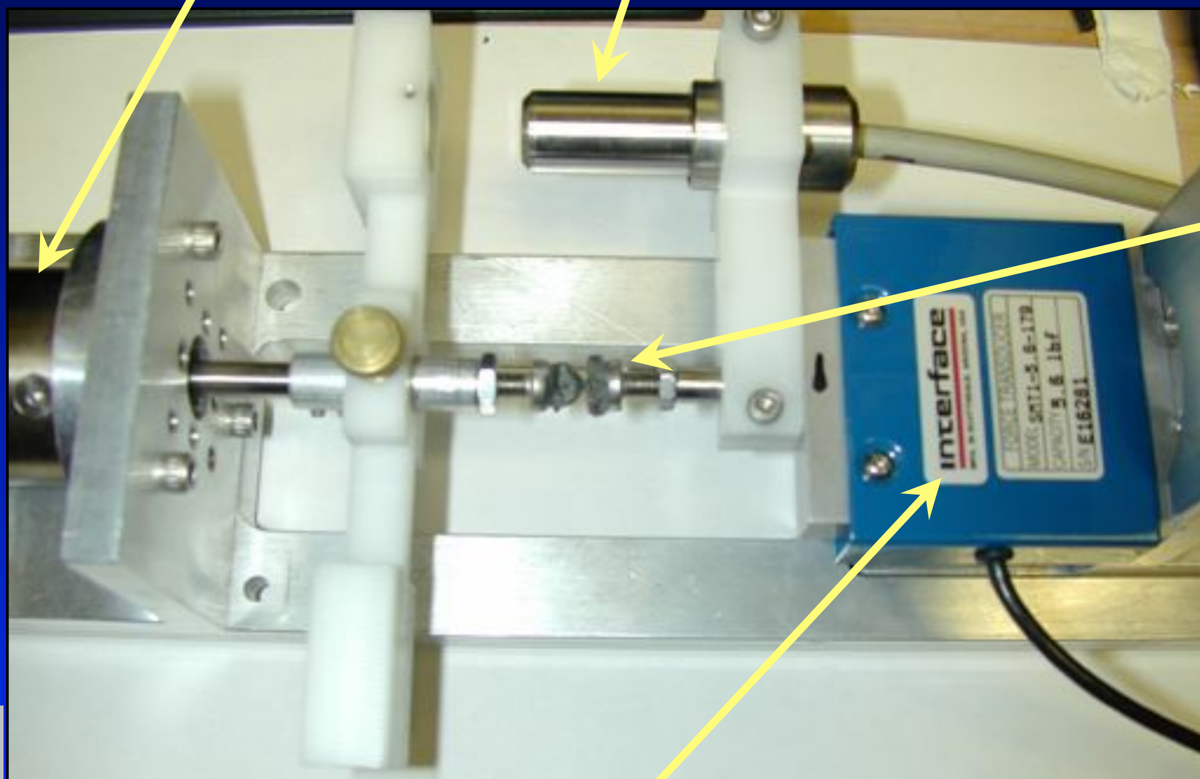

Grain pair

Load cell (0.5 or 25 N capacity)

UAF INE

Cole et al, 2007

System capabilities & waveforms

- Closed-loop (PID) control of load

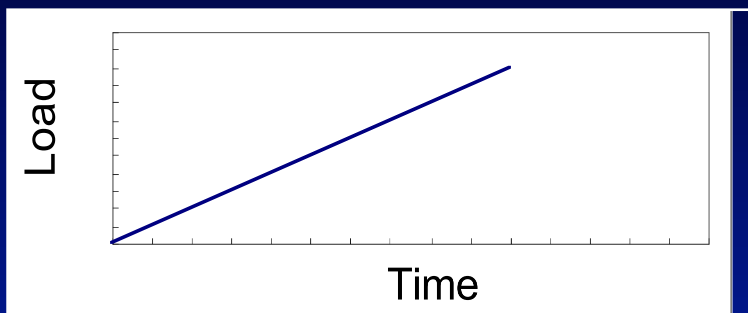

Ramp

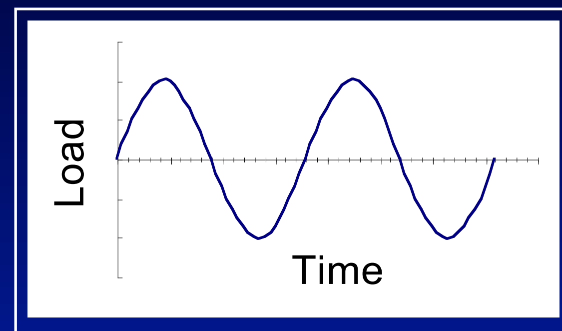

Sine

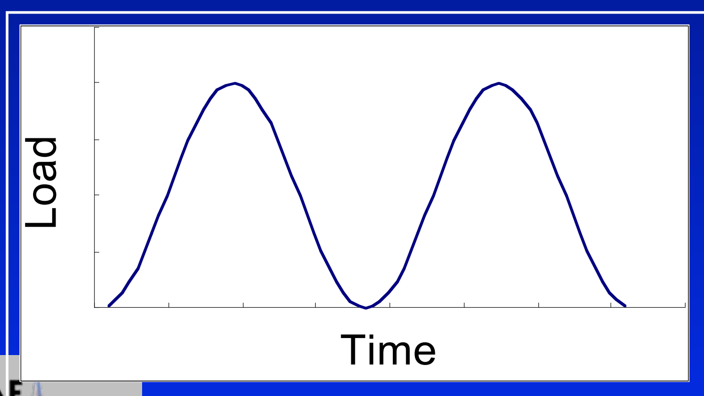

Haversine

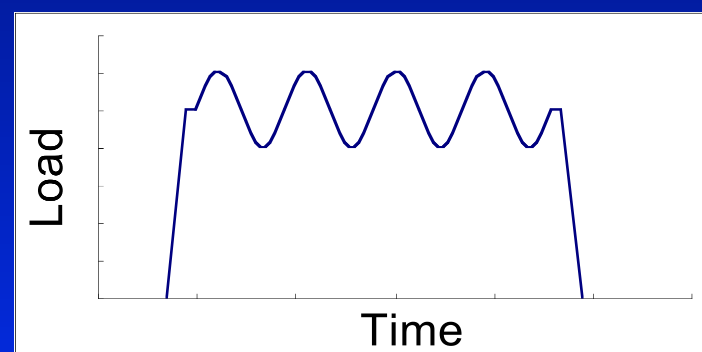

Superimposed sine wave

Normal ramp loading

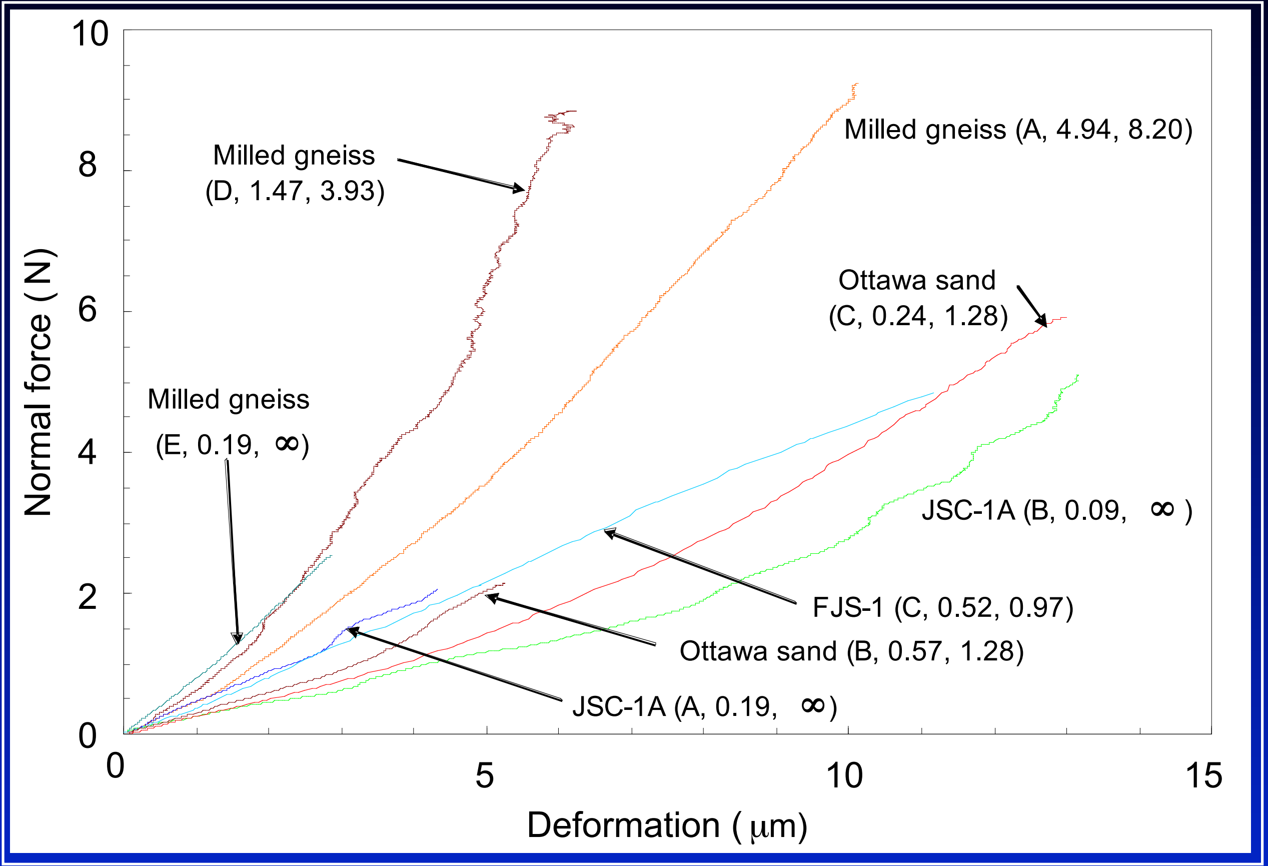

Note that most grain pairs exhibit nonlinear contact behavior.

Cole et al, 2007

Cyclic loading results – composition effects

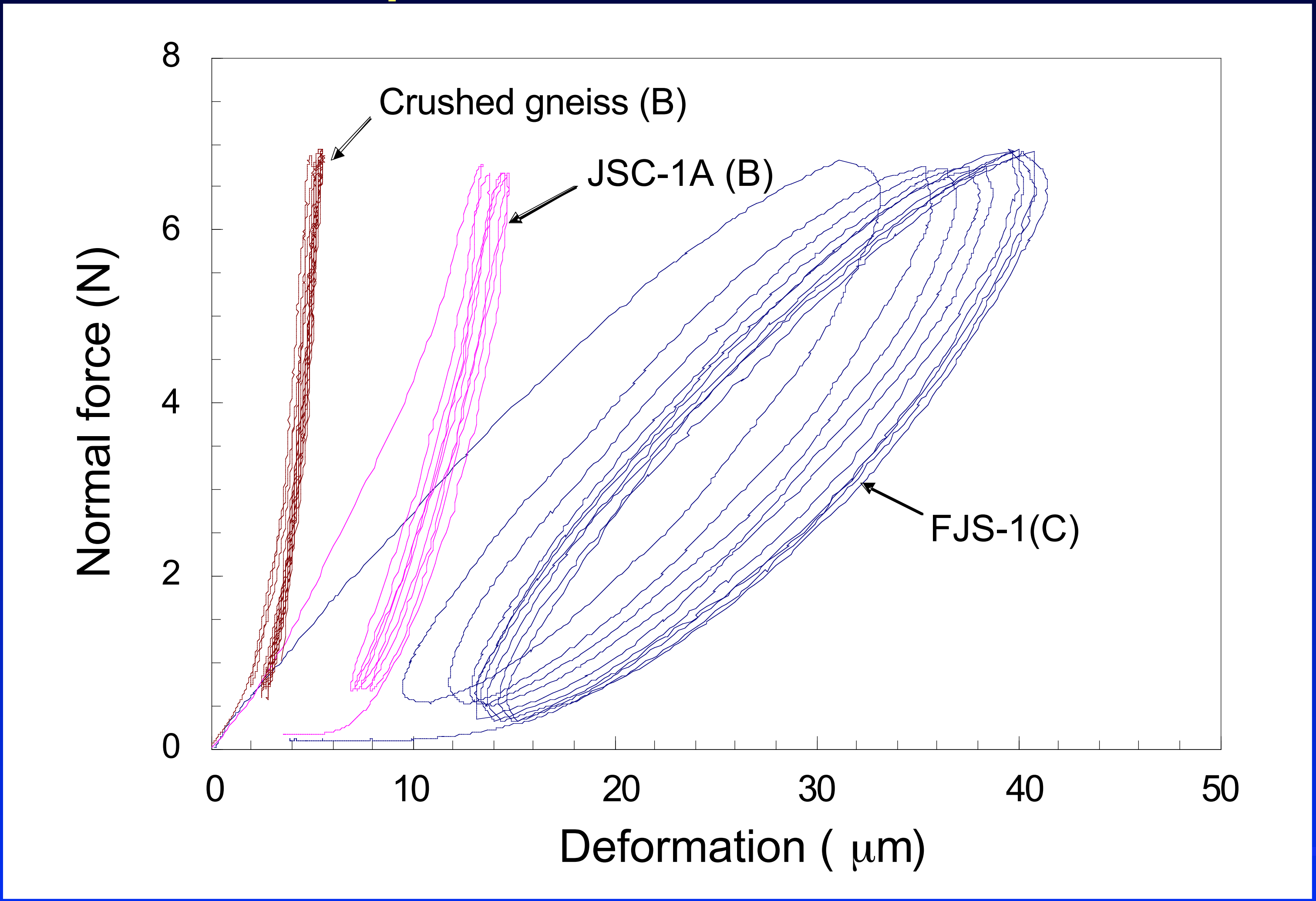

Cyclic loading results

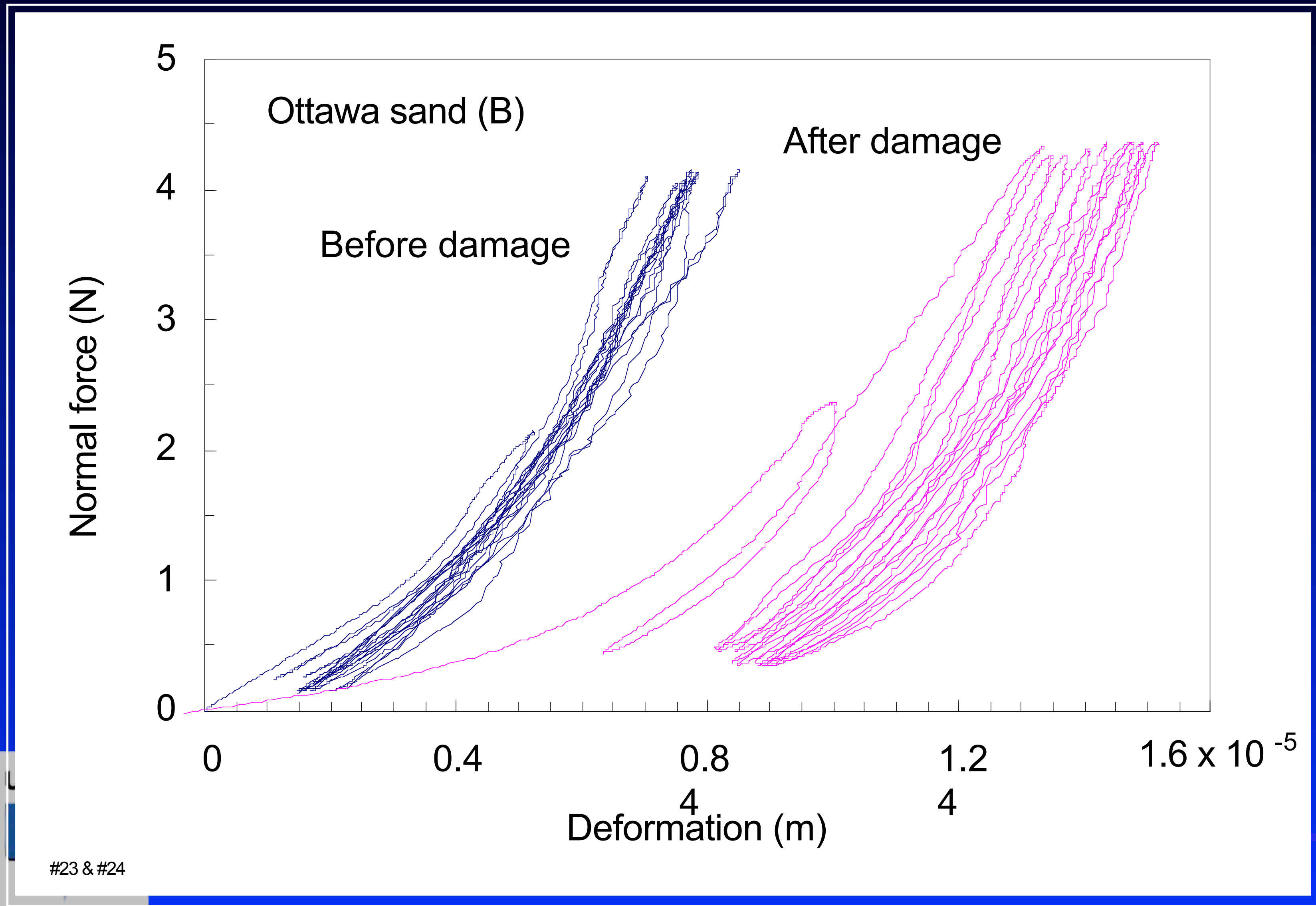

Modeling frictional loss

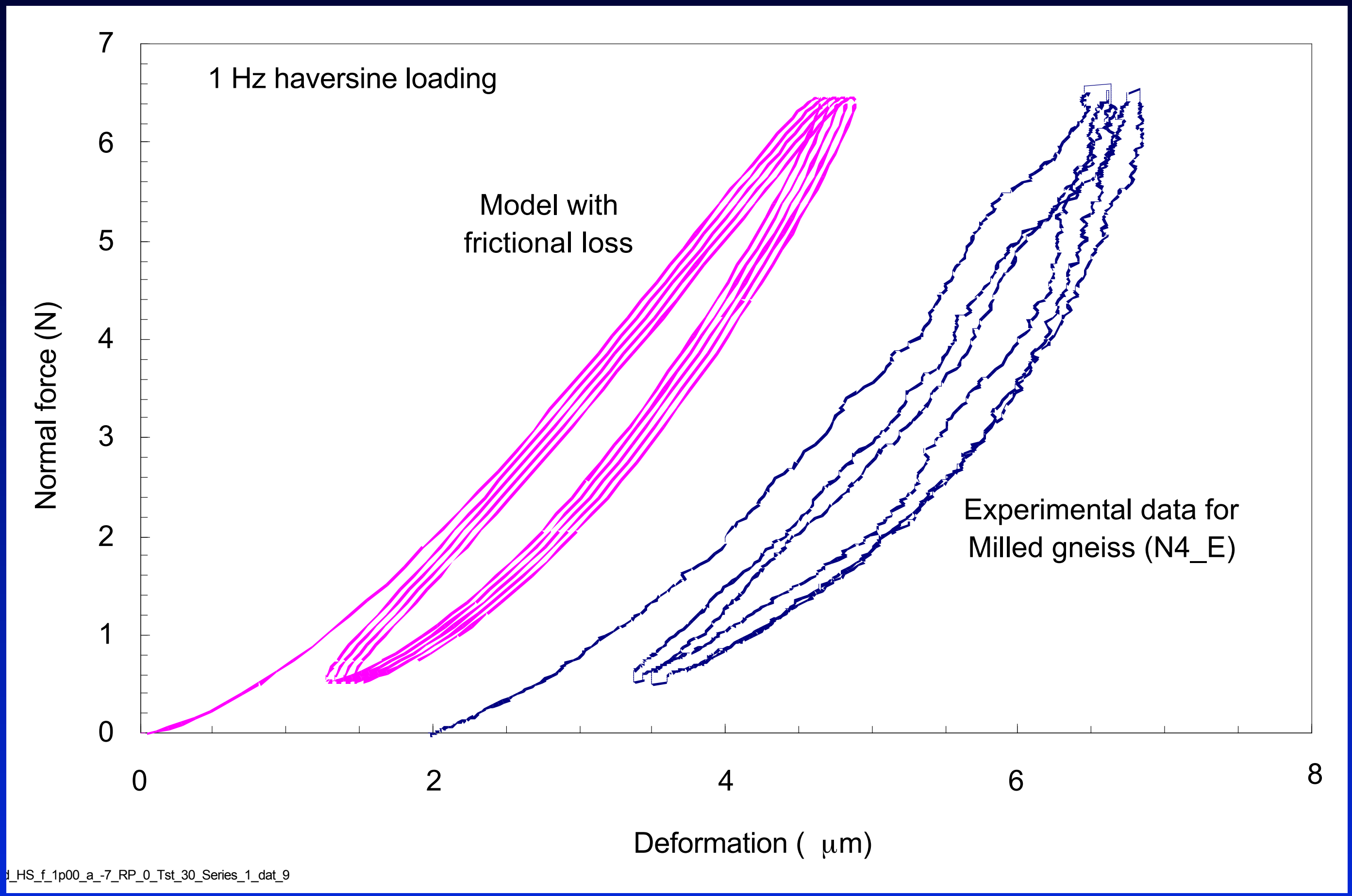

•A simple model with a normal force-dependent frictional loss and permanent deformation component adequately captures the experimentally observed behavior (Cole and Peters).

Comparison of normal contact behavior of lunar highlands plagioclase and simulant plagioclase

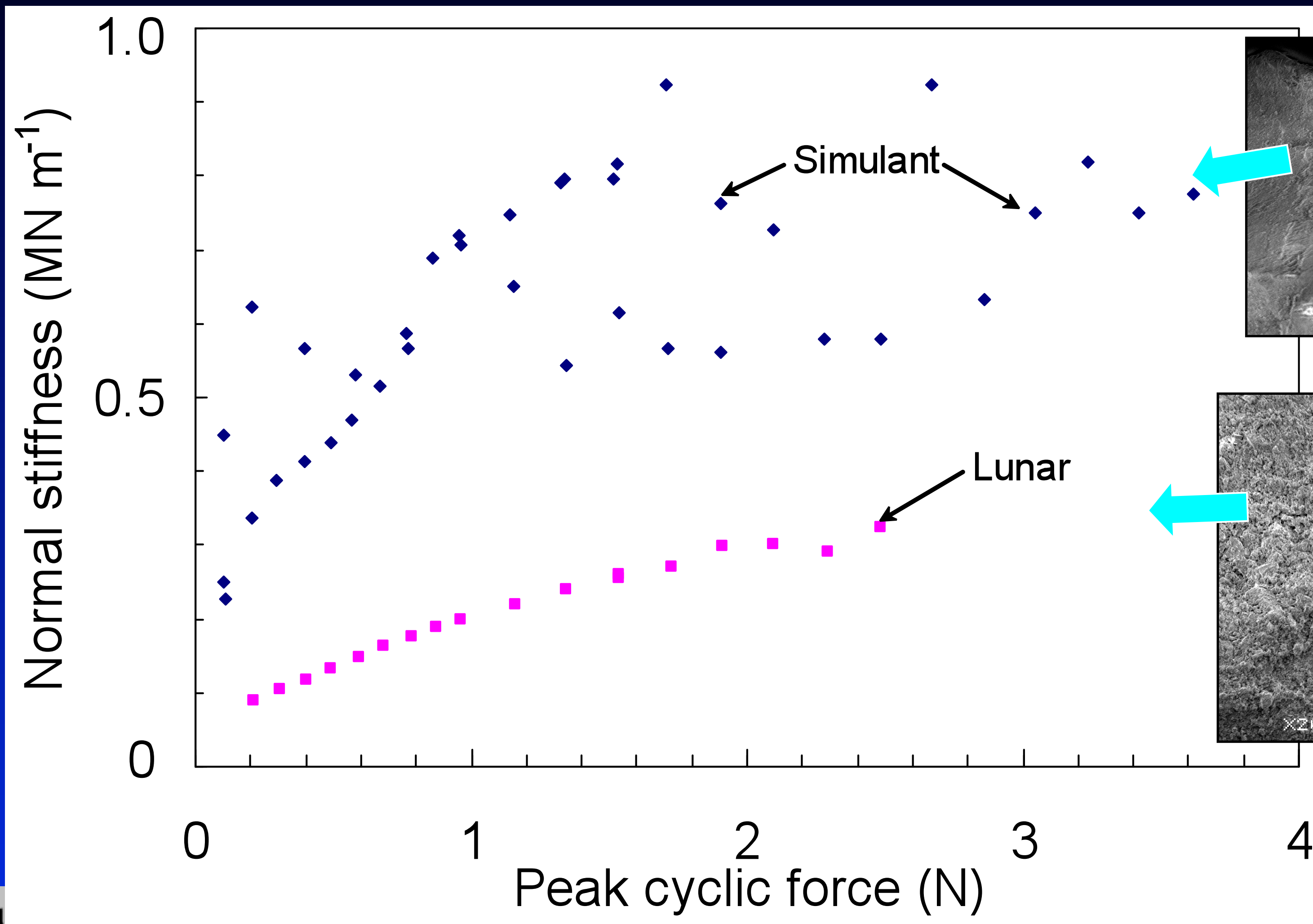

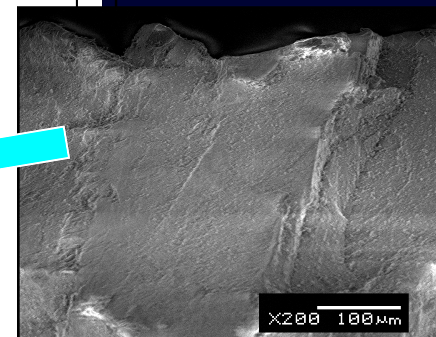

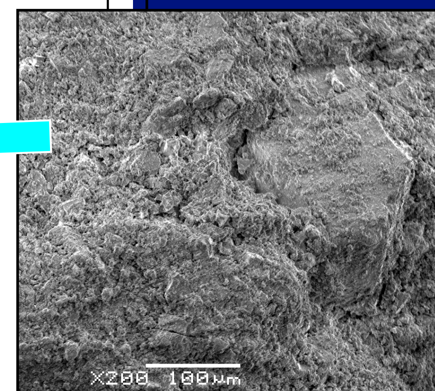

Lunar highlands plagioclase - Set 1: Grains 3-4
Simulant plagioclase (Fine) - Grains 4-7
Normal loading, 1 Hz haversine

Comparison of microstructures of lunar highlands plagioclase and simulant plagioclase

Lunar highlands plagioclase (damaged by space weathering):

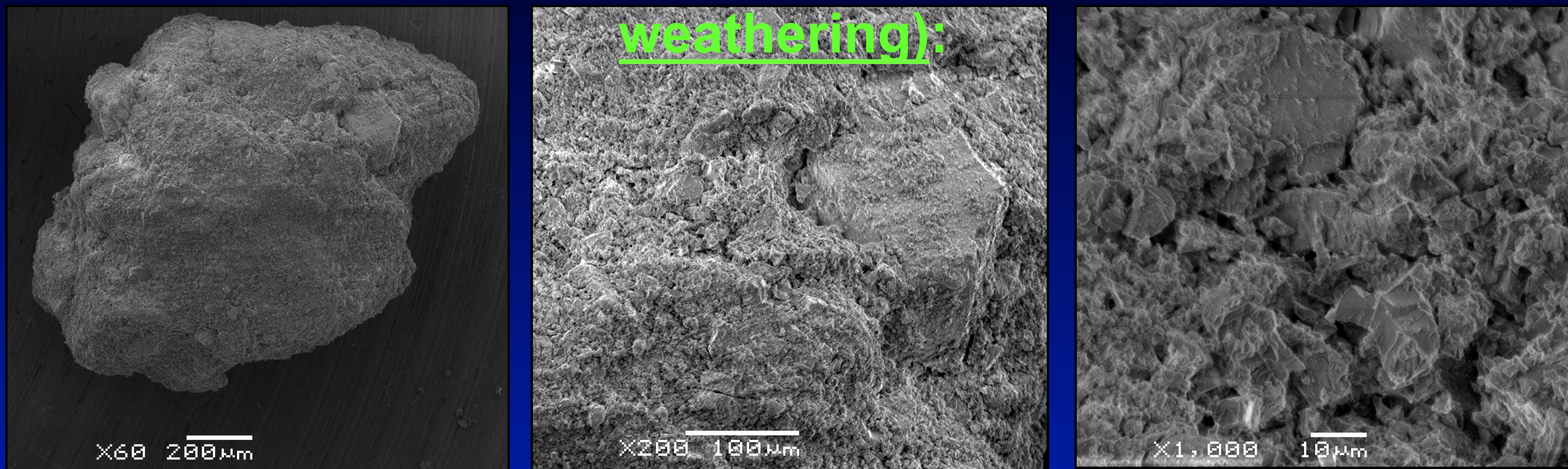

Simulant plagioclase (unweathered, robust grains):

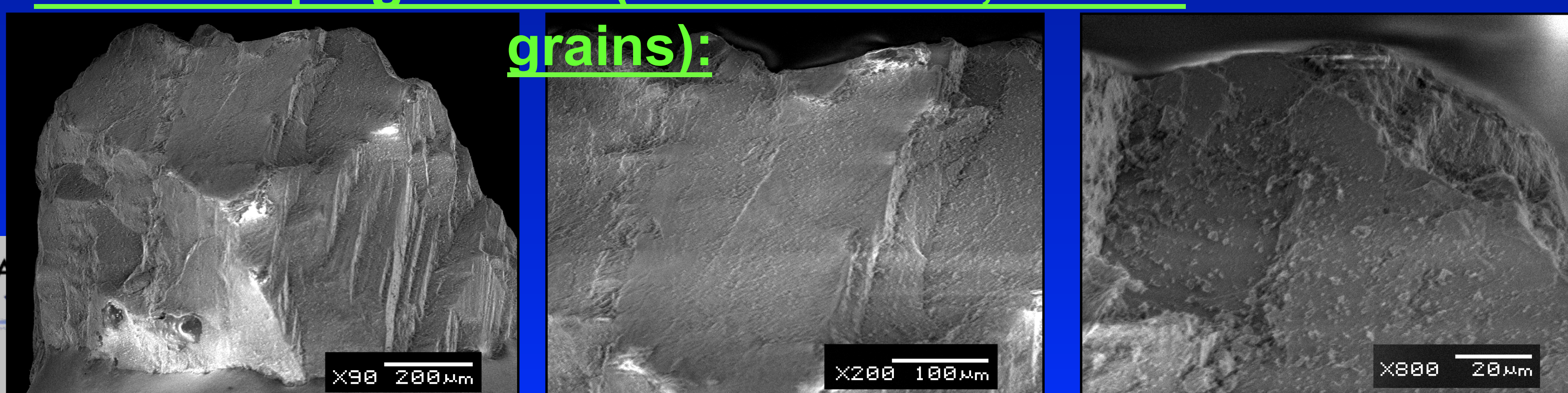

David.M.Cole@usace.army.mil

Triaxial Methods

- M. Knuth, M. Hopkins, Dave Cole

USACE ERDC-CRREL

ASCE Earth and Space 2010

Triaxial Methods

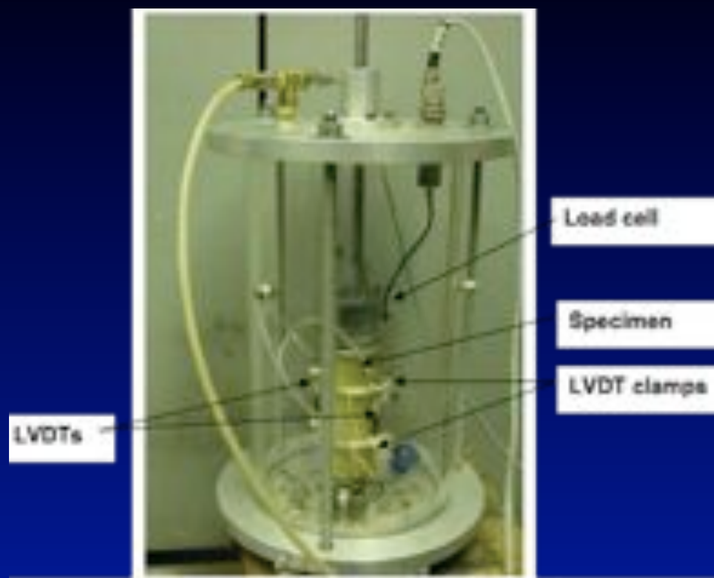

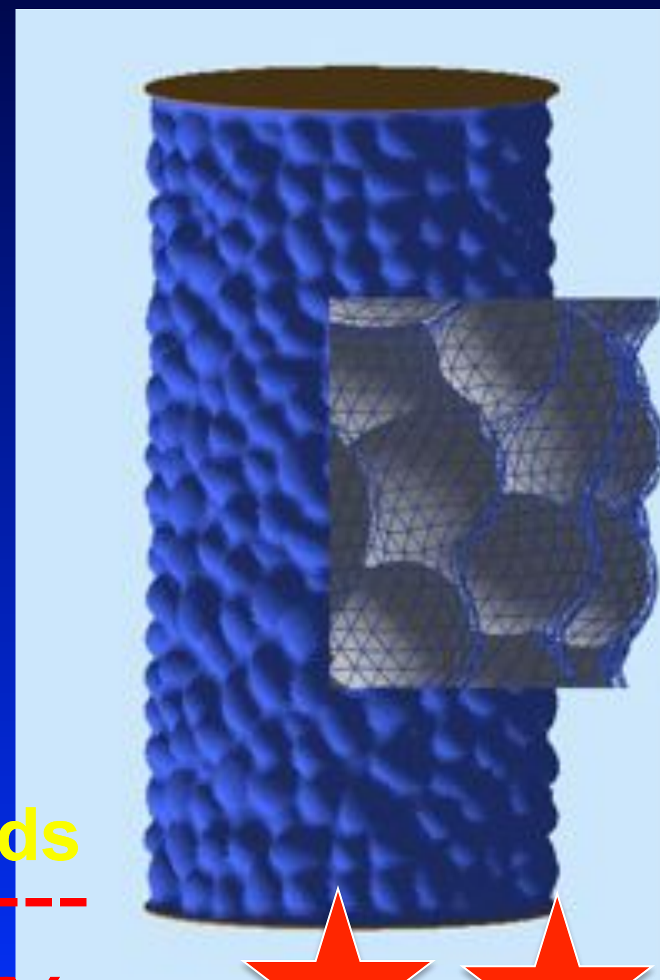

Vicksburg sand - Polyellipsoids

LEVEL OF DIFFICULTY = ★★

Triaxial Resilient Modulus Test

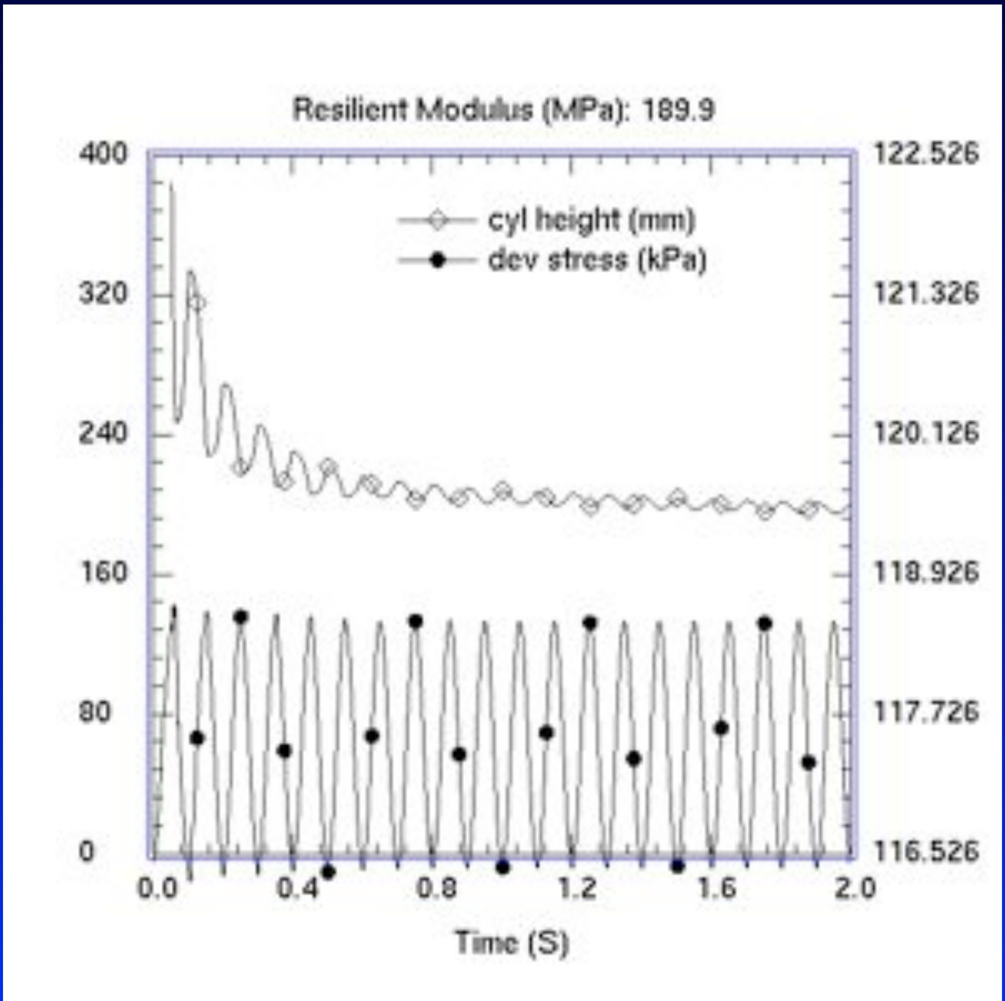

$$E_R = \sigma_d / \varepsilon$$

- Density = 1696 kg/m^3
- Confining Stress,
  σ_3 = 70 kPa
- Deviatoric Stress,
  σ_d = 140 kPa

Triaxial Resilient Modulus Test Results Versus DEM Simulation

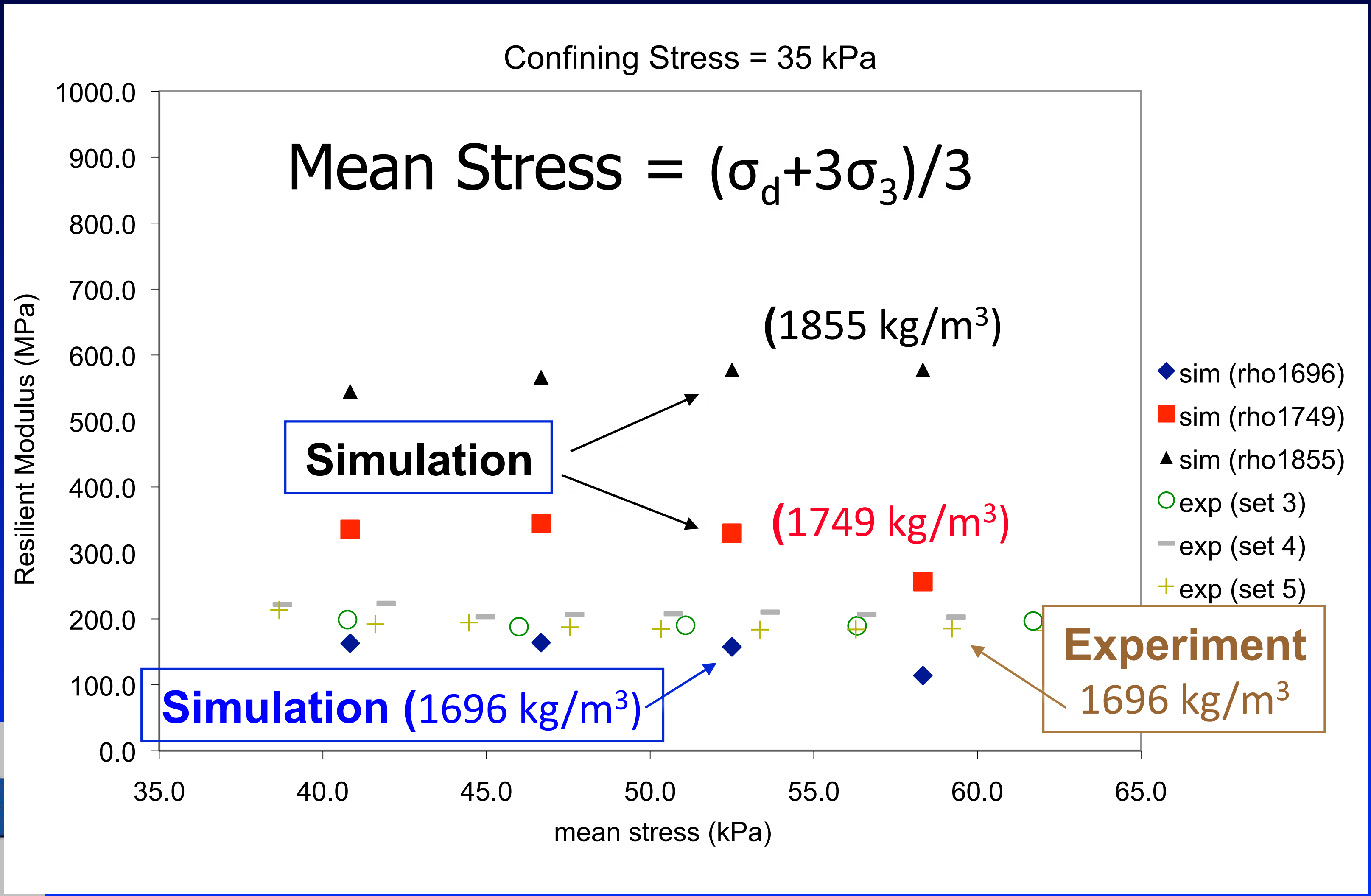

Complex Particle Shapes JSC – 1a

LEVEL OF DIFFICULTY =

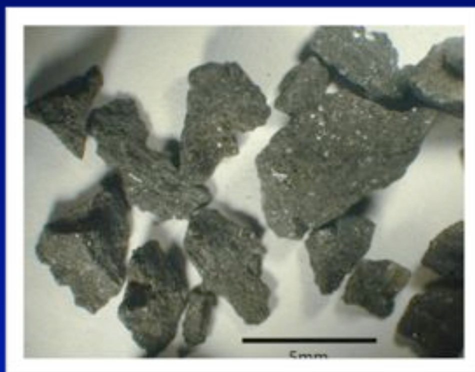

- complex angular shapes

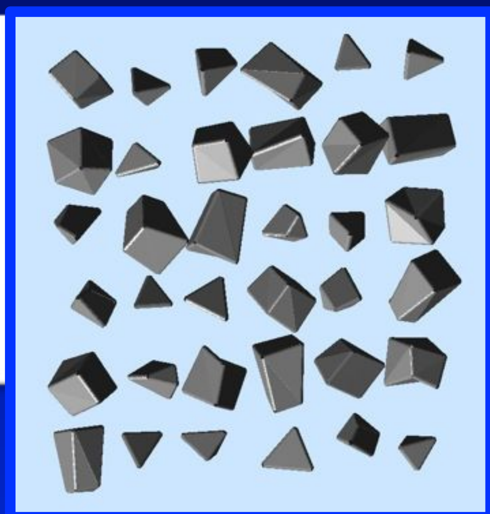

Polyhedra?

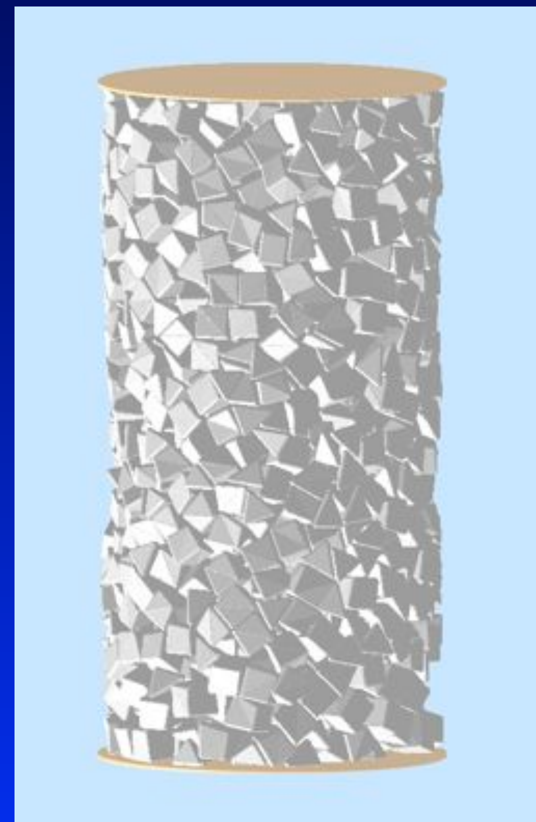

UAF INE

Case study:
Mars Exploration Rover Wheel digging Test Simulation

M. Knuth, J. Johnson, M. Hopkins, R. Sullivan, J. Moore

(Accepted – J. Terramechanics

Simulate MER digging test to determine DEM parameters

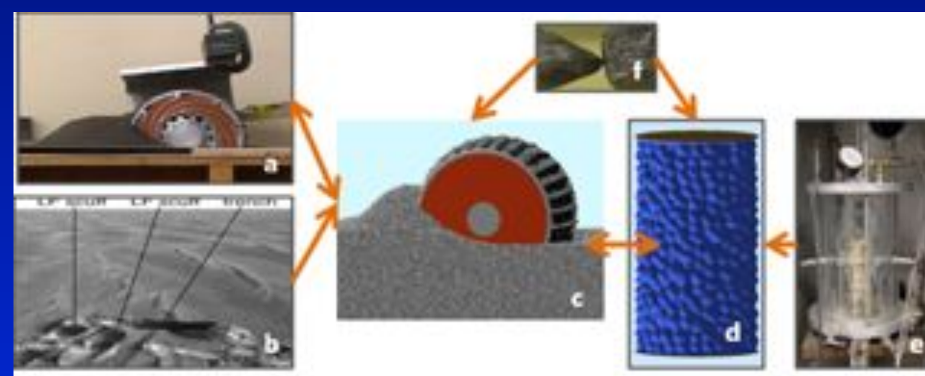

Use DEM parameters in tri-axial cell to determine soil properties – predict internal friction angle

Mars Exploration Rover Wheel Test:
Lunar Soil Simulant

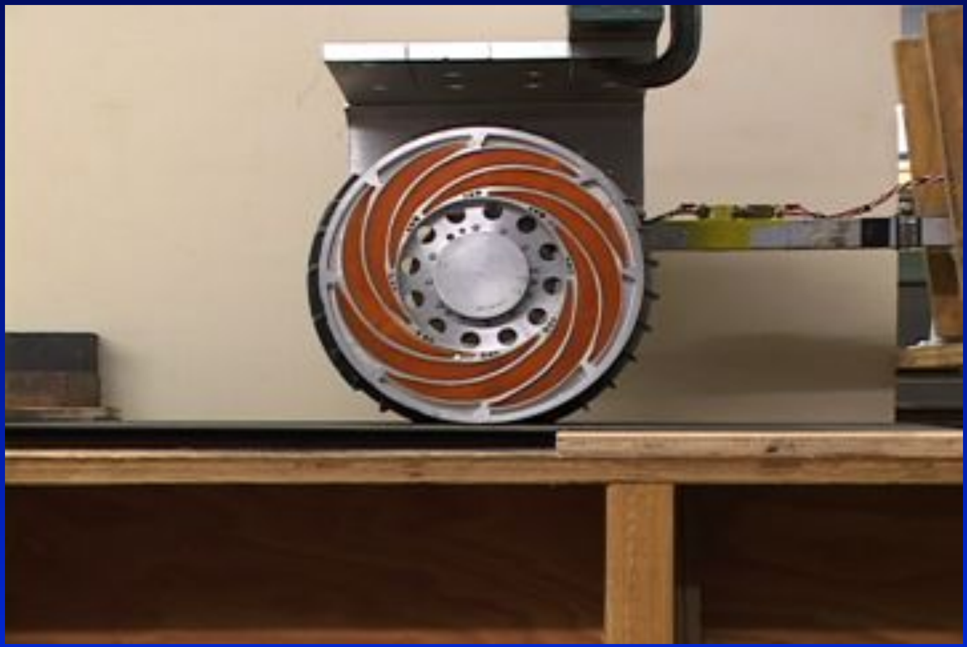

- Soil internal friction derived from:
  - Torque developed from wheel digging action
    - 36.5°
  - Angle of repose of tailings pile
    - 37.7°

Rob Sullivan's MER wheel digging test in JSC-1a

UAF INE

MER Wheel DEM Digging Simulation

- Match experimental torque and sinkage
- Derive parameters for spherical, elliptical, and poly-elliptical particles

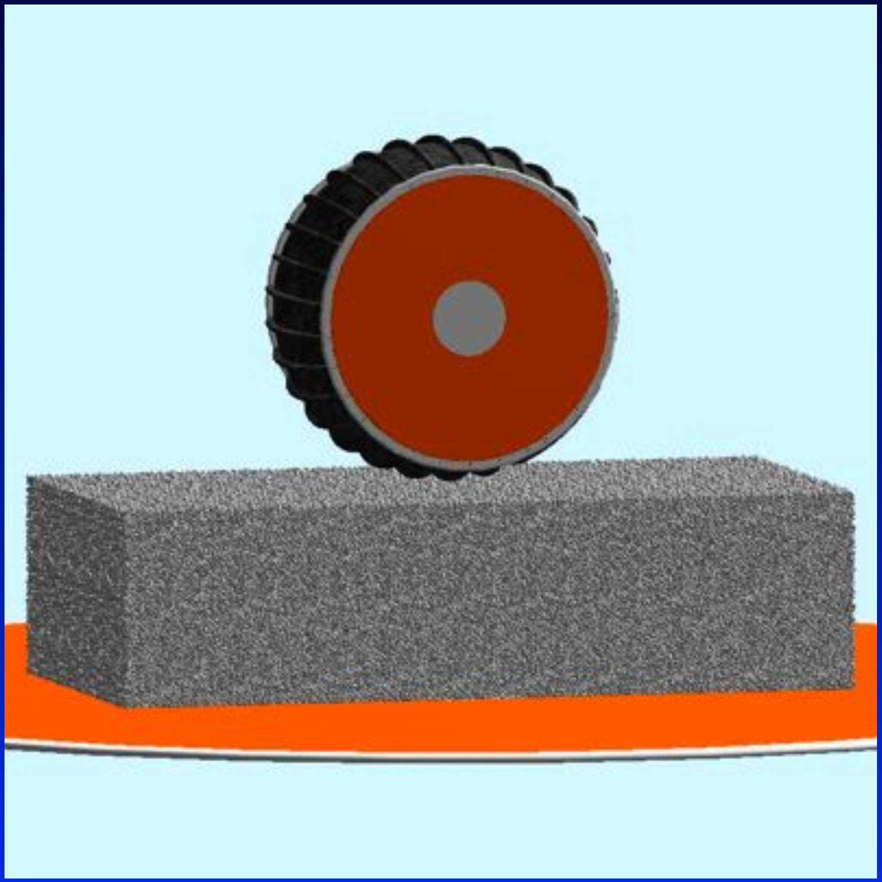

Comparison of Simulated & Measured Torque & Sinkage for Different Particle Shapes - 1

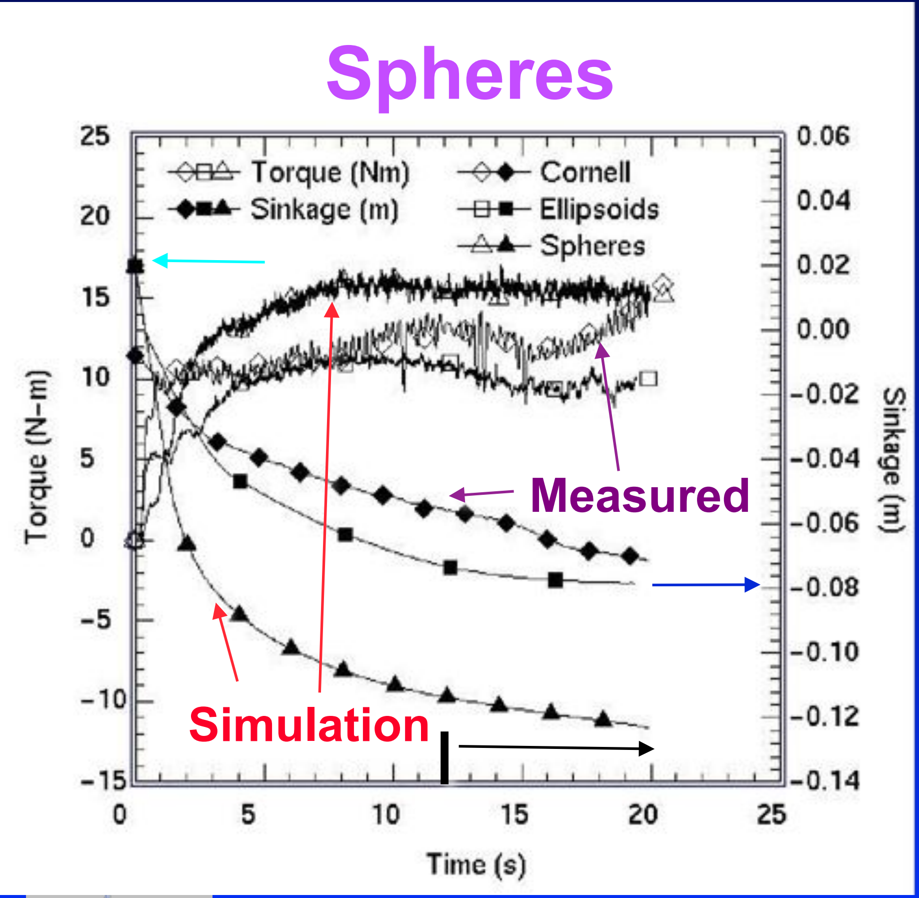

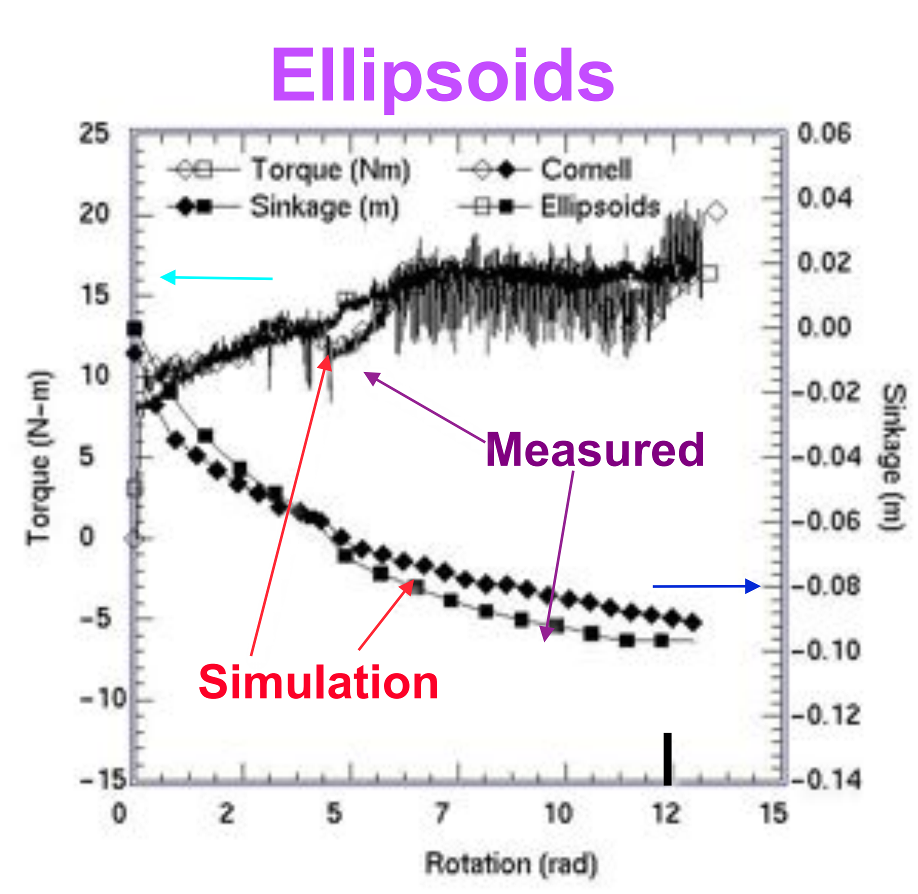

Comparison of Simulated & Measured Torque & Sinkage for Different Particle Shapes - 2

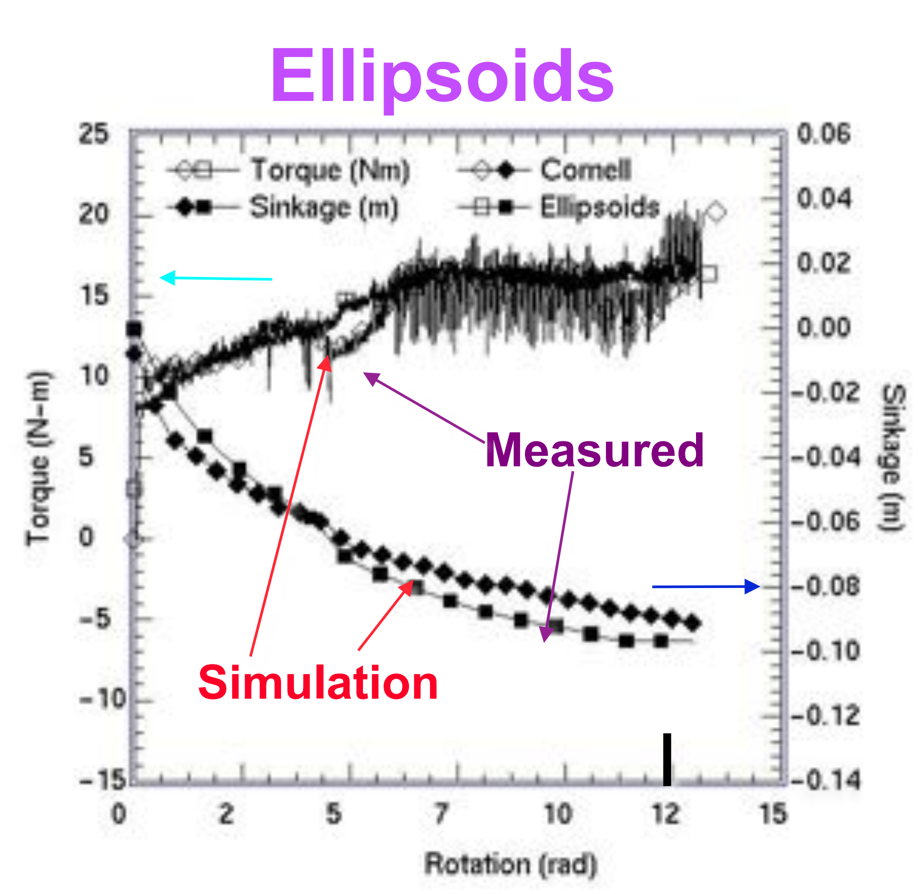

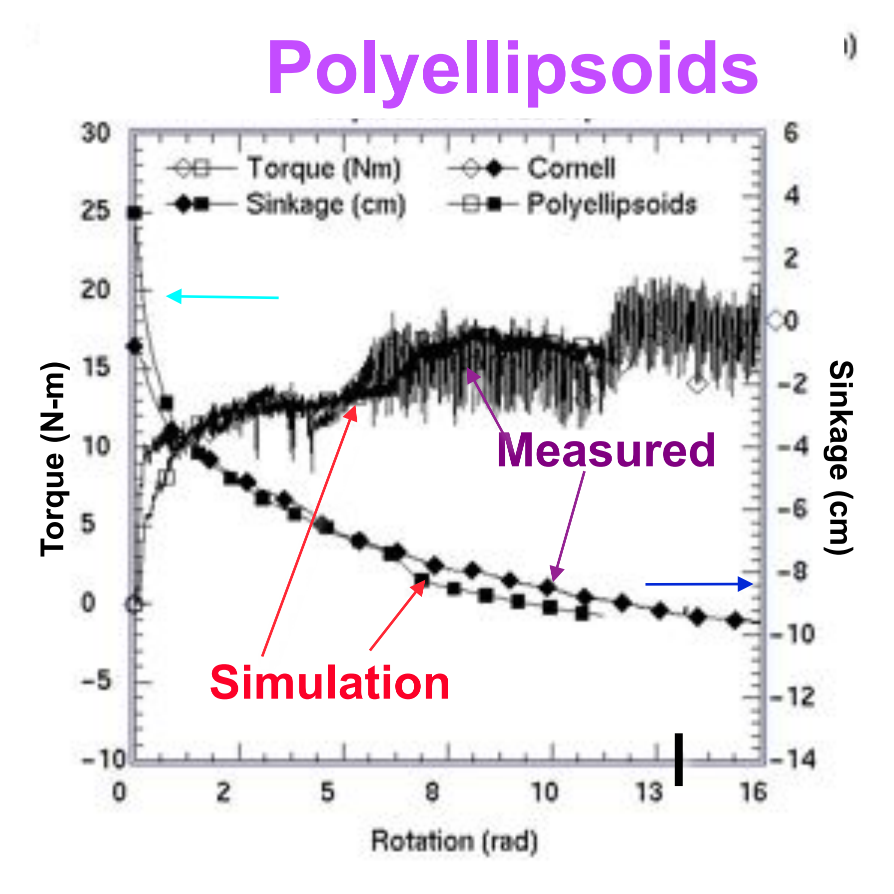

Triaxial Methods

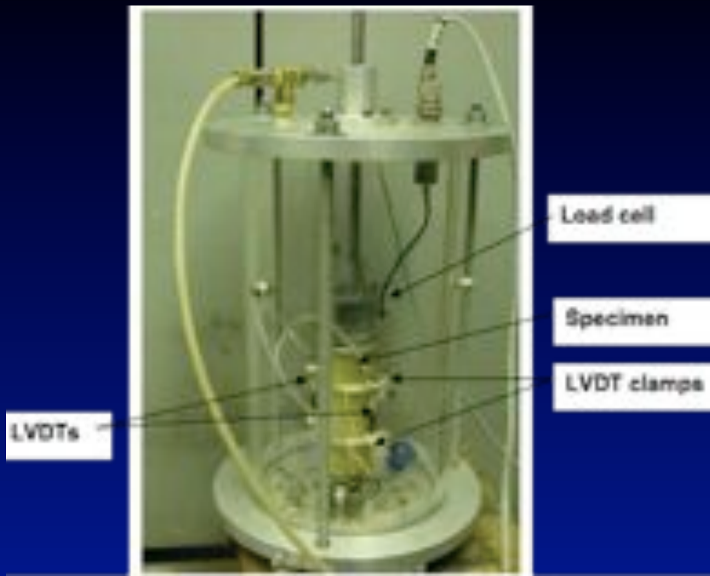

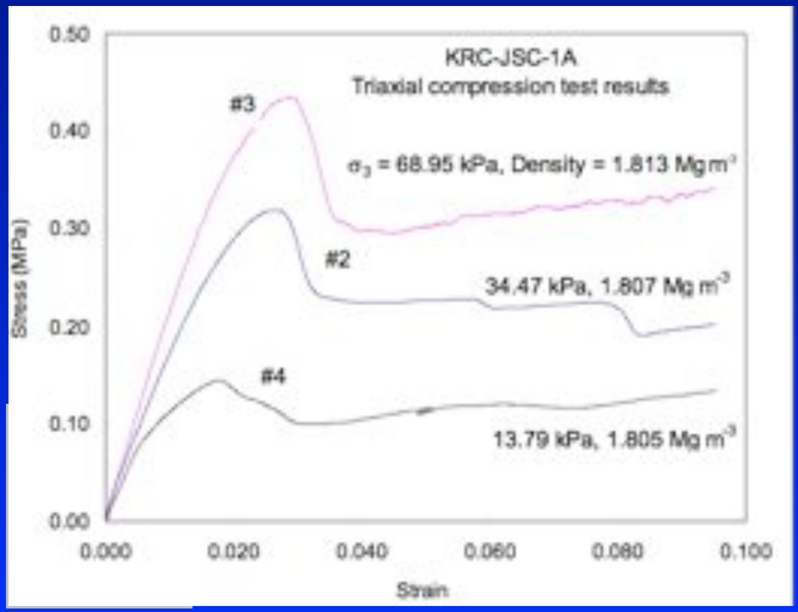

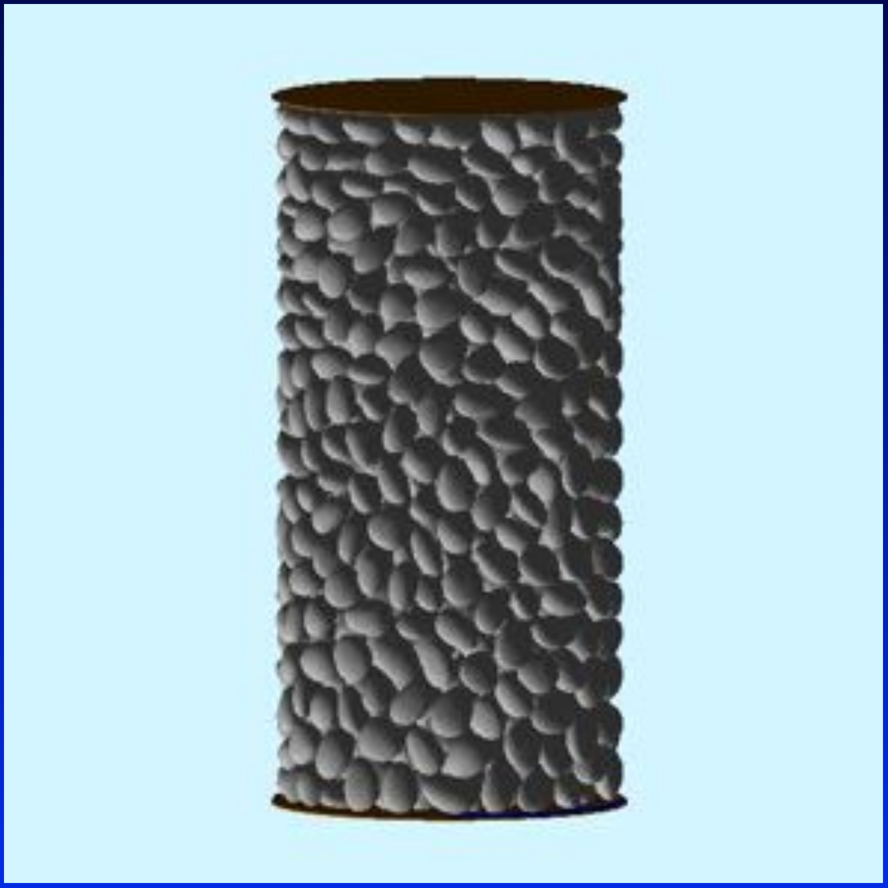

Stress Strain Behavior & Prediction of Internal Friction

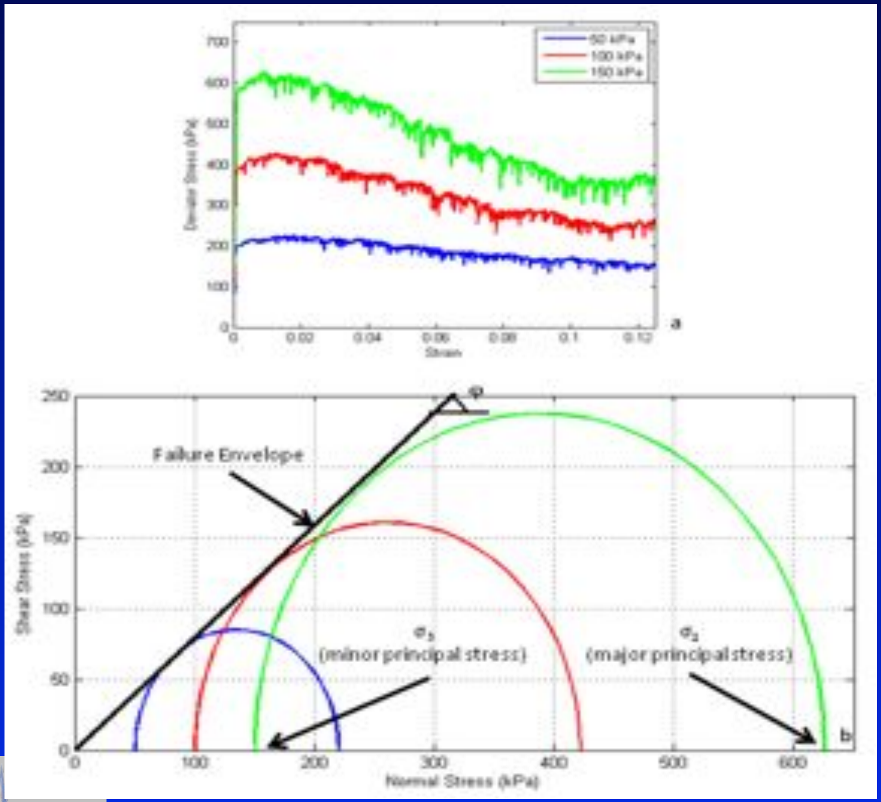

- Internal friction derived from Tri-axial cell simulation using DEM parameters from wheel digging simulation
  - 37° — 38°

UAF INE

Parameters used in the DEM Simulation

Parameter	Wheel Model	GTSC Model
Domain size (mm)	600 x 300 x 200 (l x w x d)	55 x 138 (diam x hgt)
Number of particles	361000	3000
Sphere diameter (mm)	2.5, 5	
Ellipsoid dimensions-comp 1 (mm)	6.76 x 4.38 x 4.38	
Ellipsoid dimensions-comp 2 (mm)	3.90 x 5.78 x 5.78	
Poly-ellipsoid 1 (m)[a] x 10^{-3}	3.05, 1.96, 0.366, 0.211	3.05, 1.96, 0.366, 0.211
Poly-ellipsoid 2 (m) x 10^{-3}	3.56, 1.51, 0.670, 0.422	3.56, 1.51, 0.670, 0.422
Dilating radius (mm)	0.5	0.5
Shear modulus (GPa)	0.024	30
Poisson ratio	0.3	0.3
Approx. time step (sec)	$5x10^{-5}$	$1x10^{-6}$
Particle surface friction	0.5	0.5
Gravitational constants ($m\ s^{-2}$)	1.60, 3.73, 9.81	9.81
Material density ($kg\ m^{-3}$)	2600	2600
Bulk density ($kg\ m^{-3}$)		1820
Strain rate (s^{-1})		0.02
Confining stress (kPa)		50, 100, 150
Wheel width (mm)	160	
Wheel diameter (mm)	261	
Tread and cleat radius (mm)	219	
Rover wheel mass, incl. arm (kg)	11	
Wheel rotation rate ($rad\ s^{-1}$)	0.4	

[a] Poly-ellipsoid dimensions reported as positive average radius, negative average radius, positive standard deviation and negative standard deviation.

Wheel Digging Simulation Using Polyhedra Particles

- More angular that poly-ellipse particles
- More particle interlocking
- Higher angle of repose for tailings
- Analysis still in progress

Analysis of Results 1/2

- DEM & experimentally derived internal friction are in reasonable agreement
- DEM density too high and calculated internal friction too low compared to measured values
  - @ ρ = 1820 kg/m^3 & ϕ = 41° — 48° for JSC-1A compared to 37° — 38° for DEM
  - ρ = 1820 kg/m^3 compared to ρ = 16300 kg/m^3 for Sullivan tests.

UAF INE

Analysis of Results 2/2

- Measured angle of reposed of tailings pile from test is higher that for simulation (qualitatively)
- Particle size and shape distribution limited and unrealistic compared to actual JSC-1A
- Simulation with polyhedra particles qualitatively produce higher angle of repose that poly-ellipse

Conclusions From Results 1/2

- Particle shape and contact friction important DEM parameters
- Particle size is important to reach convergence and achieve proper scale with machine components
- Particle density not important for this simulation, but is important to develop physical DEMs

UAF INE

Conclusions From Results 2/2

- Complete soil stress deformation information can be derived (validity needs verification)
- Soil properties can be determined from Machine/soil interaction data using DEM method
- DEM particle parameters can be derived from tri-axial cell soil stress-strain data to develop machine/soil interaction simulations

Overall Conclusions 1/2

- Development of a physical DEM requires coordinated experiments and simulation to derive reasonable DEM physical parameters
- Physical DEMs have the potential to accurately simulate machine/soil interactions
- Work is needed to improve DEM physical parameters (e.g. density, particle shape & size distribution, contact mechanics
- Efficient DEM codes and improved computational speeds are needed

Overall Conclusions 2/2

- Development of a physical DEM requires a alliance of specialists to
  - conduct and interpret micro-scale test, macro-scale tests, machine/soil interaction tests
  - develop physical alogrithms from test results
  - Develop computationally efficient DEM methods and simulations
  - Develop computational hardware and software solution to increase computational power

Example of Flow and DEM: Particle Entrainment